

Effects of Osteocyte-Intrinsic TGF- β Signaling in Alveolar Bone During Orthodontic Tooth Movement

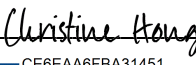
by
Jasmine Faldu

THESIS
Submitted in partial satisfaction of the requirements for degree of
MASTER OF SCIENCE

in
Oral and Craniofacial Sciences


in the
GRADUATE DIVISION
of the
UNIVERSITY OF CALIFORNIA, SAN FRANCISCO

Approved:

DocuSigned by:

CE6EAA6FBA31451... Christine Hong
Chair

DocuSigned by:

Mona Bajestan

DocuSigned by:

C84D7533F9714EF... Alice Goodwin

Committee Members

ACKNOWLEDGEMENTS

This study would not have been possible without a supportive and collaborative team. I would first like to thank Dr. Christine Hong for giving me the opportunity to work with her. Her scientific vision, continuous encouragement, and mentorship is what made this project possible. The support of Dr. Mona Bajestan and Dr. Alice Goodwin also contributed to my understanding of the scientific process and executing that knowledge throughout this project. A thank you for giving their time to be on my thesis committee.

I would like to thank and recognize Dr. Tamara Alliston for sharing her wealth of knowledge in bone biology and collaborating with her lab team. Her lab provided the mice for this study which made it possible to start answering these scientific questions to impact the practice of orthodontics.

The wonderful Jinsook Suh served as my personal mentor every step of the way. Her understanding of translational research and extensive expertise with studies like mine made her invaluable to the mission of the project. I cannot thank you enough for your continuous support.

I would like to express gratitude to Dr. Sumit Yadav for giving his time to provide guidance with his extensive experience in mouse model orthodontic tooth movement.

This project was made possible with the great support of my co-resident Albert Ngo, who spent many days and nights collaborating with me to make this project move forward. I would also like to thank my colleagues Jihee Yoon and Gregory Pavlos for their collaboration, input, and contributions to this project.

Every long-term goal takes time, patience, and support. This would not have been possible without my personal support system of my family. Your curiosity about this project helped fuel me to keep moving forward. A very special individual who has unwavering love and

support throughout this project that I would like to acknowledge is Niromal Perera, my fiancé.

Thank you for always making sure that I have my ID to check on the mice in the LARC facility.

ABSTRACT

Effects of Osteocyte-Intrinsic TGF β Signaling in Alveolar Bone During Orthodontic Tooth

Movement

by

Jasmine Faldu

Objectives: In this study, orthodontic tooth movement (OTM) was applied to T β RII $occy^{-/-}$ mice to elucidate the role of osteocyte-intrinsic TGF β signaling in alveolar bone remodeling during tooth movement.

Methods: Osteocyte-specific TGF β receptor II knockout mice were examined to study whether TGF β signaling in osteocytes is required for alveolar bone remodeling induced by orthodontic tooth movement forces. Male and female mice underwent OTM appliance delivery under general anesthesia. OTM was induced by a coil spring appliance that was ligated and bonded to the maxillary left first molar and the maxillary incisors. The mice underwent OTM for 14 days until euthanized. Then *ex vivo* MicroCT was used to measure OTM, bone mineral density, bone volume fraction, and bone to tissue volume ratio. The study included eight groups of mice: male and female control (CTRL), and male and female knockout (KO) in Dmp1-Cre $^{+/-}$;Tbr2 $^{fl/fl}$ group and Dmp1-Cre $^{-/-}$;Tbr2 $^{fl/fl}$ groups. Control mice also underwent *ex vivo* MicroCT and was used to measure bone mineral density, bone volume fraction, and bone to tissue volume ratio for comparison.

Results:

Our results shed light on some striking differences between genders as well as the properties of alveolar bone versus the reported properties of long bone in the literature. Non-experimental baseline group (no OTM) there was no statistically significant difference in bone quality between

genotypes within the same gender. However, at baseline there was a statistically significant difference in alveolar bone quality between females and males. We found utilizing orthodontic tooth movement linear measurements that there was a large variation in OTM in the male *Dmp1-Cre^{+/-};Tbr2^{fl/fl}* group, which could be explained by the disruption of the down signaling cascade when TGF β is not functioning. Also, in males we found a decreased BV/TV and BMD in alveolar bone in the OTM group compared to the gender-matched controls.

Conclusions:

This study furthers our understanding of the role osteocytes may play in the process of bone remodeling during OTM. Our preliminary data were promising and increasing the sample size will help support further scientific discovery and clinical applications. The OTM mouse model utilized in this study is reliable and reproducible for long term studies. The significant differences in bone quality between males and females illustrates the importance of separating experimental groups by sex, genotype, and phenotype, and provides potential clinical insight as to how males and females alveolar bone may respond differently to loads than the long bones. The OTM protocol in mice will continue to assist in scientific research to help us learn how to optimize orthodontic treatment and develop innovations in the field.

TABLE OF CONTENTS

A: INTRODUCTION	1
A1: Preface and Specific Aims	1
A2: Biology and Biomechanics of Tooth Movement	3
A3: Role of Osteocytes During Orthodontic Tooth Movement	6
A4: Understanding the Role of TGF β signaling in bone biology	8
B: Materials and Methods	10
B1: Background	10
B2: Funding	11
B3: Sample Size	11
B4: Subjects	12
B5: Sedation and Pain Control	12
B6: Orthodontic Appliance Treatment	13
B7: MicroCT Protocol	14
B8: MicroCT Protocol and Analysis	15
B8.a: Orientation	15
B8.b: Linear Distance of Orthodontic Tooth Movement	22
B8.c: Volumetric Measurements	28
B9: Statistical Analysis	42

C: RESULTS	42
C1: Final Sample Size	42
C2: MicroCT Analysis Results	42
D: DISCUSSION	48
E: FUTURE DIRECTIONS	52
F: LIMITATIONS	52
G: CONCLUSIONS	53
H: REFERENCES	54

LIST OF FIGURES

- Figure 1:** This sagittal cross-section of the MicroCT image of a baseline mouse sample illustrates the robust nature of the maxillary incisor tooth root. The crown to root ratio for the incisors is favorable to induce OTM 13
- Figure 2:** Illustrates the schematic view on the right and in-vivo on the left of the orthodontic appliance with all the components: ligature ties, coil spring, composite and bonding material. 14
- Figure 3:** Graphical representation of the baseline groups split by male and female for Dmp1-Cre^{+/-};Tbr2^{fl/fl} and Dmp1-Cre^{-/-};Tbr2^{fl/fl} groups. No statistically significant findings were noted. 43
- Figure 4:** A. Baseline gender comparison for BV/TV in Dmp1-Cre^{-/-};Tbr2^{fl/fl} mice.
B. Baseline gender comparison for BMD in Dmp1-Cre^{-/-};Tbr2^{fl/fl} mice.
C. Coronal cross-section of maxillary left side first molar at the level of the furcation area in female Dmp1-Cre^{-/-};Tbr2^{fl/fl} mice. D. Coronal cross-section of maxillary left side first molar at the level of the furcation area in male Dmp1-Cre^{-/-};Tbr2^{fl/fl} mice. 44
- Figure 5:** A. Baseline gender comparison for BV/TV in Dmp1-Cre^{+/-};Tbr2^{fl/fl} mice.
B. Baseline gender comparison for BMD in Dmp1-Cre^{+/-};Tbr2^{fl/fl} mice. C. Coronal cross-section of maxillary left side first molar at the level of the furcation area in female Dmp1-Cre^{+/-};Tbr2^{fl/fl} mice. D. Coronal cross-section of maxillary left side first molar at the level of the furcation area in male Dmp1-Cre^{+/-};Tbr2^{fl/fl} mice. 44
- Figure 6:** Graphical representation of orthodontic tooth movement linear measurements between genotypes when split by gender. 45
- Figure 7:** Female control and OTM groups comparison between genotypes for bone quality. 46
- Figure 8:** Male control and OTM groups comparison between genotypes for bone quality. 46

Figure 9: Graphical comparison of BV/TV and BMD between genders within the same genotype after 14 days of orthodontic tooth movement.

47

LIST OF TABLES

Table 1: Breakdown of samples included in the statistical analysis.

42

LIST OF ABBREVIATIONS

BMD – bone mineral density

BV/TV – bone volume fraction

CTRL – control mouse group

KO – knockout mouse line

OTM – orthodontic tooth movement

PDL – periodontal ligament

PLR – perilacunar/canalicular remodeling

RANKL – receptor activator of nuclear factor κ - β ligand

TGF β – Transforming Growth Factor - beta

TBRII – TGF β receptor II

WT – wildtype mouse line

A: INTRODUCTION

A1: Preface and Specific Aims

Orthodontic tooth movement (OTM) induces an intricate biological response to yield bony remodeling to allow changes in the tooth position. Orthodontists rely on an understanding of bone biology to successfully move teeth to create esthetic smiles and healthy occlusion. Bone is a very dynamic organ, and it is known to be a rigid body tissue consisting of cells embedded in an abundant, hard intercellular material. The bone of focus for this investigation is alveolar bone where the dentition is housed. The integrity of alveolar bone is controlled by hormones and proteins secreted by hematopoietic bone marrow cells and bone cells. There are known key local regulators within alveolar bone such as platelet derived growth factor, insulin growth factors, transforming growth factor- β (TGF β), and bone morphogenetic proteins (BMP) [1].

Currently, there is a consensus on the role of osteoblasts, the mesenchymal bone-forming cells, and osteoclasts, the hematopoietic bone-resorbing cells, in the process of bone remodeling during OTM. When orthodontic force is placed on a tooth, bone is produced on the tension side by osteoblasts and bone is resorbed on the compression side of the PDL by osteoclasts [2] [3] [4]. However, there is limited knowledge on the role of osteocytes, the mechanosensory cells within the bone, even though osteocytes account for the largest proportion of cells within the matrix of the bone [5] [6]. Osteocytes are a cell type that are derived from osteoblasts and are localized within the mineralized bone matrix. The literature suggests osteocytes play a role in tooth movement in response to orthodontic forces [7] [8] [9]. Osteocytes have channels or canaliculi within the bone matrix to allow them to communicate with cells on the surface that are not in direct contact. Different loads and stresses within the bone matrix are sensed by osteocytes and

signals are sent to surrounding osteoclasts and osteoblasts to act. The modulation of bone remodeling is led by osteocytes to maintain bone quality and mineral homeostasis [10].

Foundational investigations by our group have led to the understanding that TGF β signaling regulates mechanosensing, RANKL and Sclerostin production, and perilacunar remodeling (PLR) in long bones in osteocytes [7] [11] [12]. In long bones, TGF β has been studied in greater detail and shown to stimulate osteocytes to increase RANKL production which leads to osteoclastogenesis [1] [13]. Since PLR is hard to define in long bone, which is a much broader and not confined environment in the human body, an avenue to learn more is by studying alveolar bone. A more controlled environment for OTM, which helps focus on the nature of the bony changes and contribute further to the study of bone biology and OTM. The concentration of this study is on osteocytes and how the lack of TGF β signaling from these cells may impact the surrounding alveolar bone structure and OTM.

Hypothesis: We hypothesize that defective TGF β signaling in osteocytes impairs alveolar bone remodeling and decreases OTM rate.

AIM 1: To develop a protocol for OTM in a mouse model.

In Aim 1, we will develop a design for OTM in mice. The orthodontic appliance will be ligated to the maxillary left first molar and both central incisors. This design will allow for mesial movement of the maxillary first molar. The forces used for the OTM should be consistent and reproducible.

Primary outcome measures: An orthodontic appliance that can induce OTM and is stable throughout the 14 day experimental time period. **Success criteria:** Successful placement of an orthodontic appliance that is stable and does not interfere with the ability of the mouse to eat, drink, and breathe.

AIM 2: To determine the extent to which loss of osteocyte-intrinsic TGF β signaling affects OTM rate.

In Aim 2, we will use the OTM model developed in Aim 1 to complete a study in mice with an experimental period of 14 days. OTM will be measured on microCT images. **Primary outcome measures:** Maintained placement of orthodontic appliance *in vivo* for 14 days using OTM mouse model optimized in **AIM 1. Success Criteria:** Observation of tooth movement on the left side versus the control samples supported by *ex vivo* microCT analysis.

AIM 3: To assess the extent to which loss of osteocyte-intrinsic TGF β signaling impacts alveolar bone remodeling.

In Aim 3, we will use the OTM model developed in Aim 1 to complete a study in mice with an experimental period of 14 days. Bone mineral density (BMD) and bone volume fraction (BV/TV) will be measured on microCT images. **Primary outcome measures:** Measured the bone mineral density and bone volume fraction on *ex vivo* MicroCT in the furcation area to highlight changes in the alveolar bone. **Success Criteria:** Observation of bone remodeling on the left side versus the control samples supported by *ex vivo* microCT analysis.

A2: Biology and Biomechanics of Tooth Movement

Understanding the biology and biomechanics of tooth movement is the cornerstone of an orthodontist's knowledge to successfully move teeth. An orthodontist relies on human biological processes to take place to induce tooth movement for a healthier, stable occlusion. Orthodontic forces trigger a cascade of events in order to move teeth within the alveolar bone. During OTM, mechanical force is placed on the tooth which translates to the periodontal ligament (PDL) as tension or compression. This leads to extravasation of vessels, chemo-attraction of inflammatory cells, and recruitment of osteoblast and osteoclast progenitors [14]. The PDL is the supporting

anatomy that connects the tooth to the alveolar bone and is the reason tooth movement is possible. Collagenous fiber bundles, cells, neural and vascular components, and tissue fluids make up the dense fibrous connective tissue PDL structure, which is about 0.2mm wide circumferentially around the roots of the tooth [15]. PDL fibers are connected to the alveolar bone and cementum through the lamina dura. There are many cell types that play important roles. The focus for establishing the biology will be on osteoblasts, osteoclasts, and osteocytes [1]. The role of osteoblasts and osteoclasts in OTM is well known [16] [17] [18]. On the tension side, osteoblasts are present depositing bone, and on the compression side, osteoclasts are present resorbing bone. These different areas of bone building and bone destruction is what leads to bony remodeling.

Although there are three phases of tooth movement established by Burstone in 1962, initial phase, lag phase, and post lag phase, this study focuses on the time frame that captures the initial phase of OTM within the first two-week period [19]. OTM is a dynamic process that can be explained by several proposed mechanisms. Three theories that are often referenced are the Pressure-Tension Theory, Bone-Bending Theory, and Biological Electricity Theory. The pressure-tension theory supports that the tooth can move because of the pressure and tension created within the PDL. Due to the difference of force in the micro-environment it alters the blood flow in the periodontal ligament. Therefore, there is less oxygen on the compression side and more oxygen on the tension side [20]. Cellular activity and differentiation can be impacted directly or indirectly due to these changes in the PDL leading to a cascade of molecular events. If the orthodontic force exceeds that of the capillary blood pressure, then tissue necrosis can initiate on the pressure side with limited oxygen [21]. As the blood flow reduces, some cells will undergo apoptosis or necrosis. These cell deaths trigger an acute inflammatory response where

chemokines are released into the PDL [22]. During orthodontic movement, the chemokines known as monocyte chemo attractant protein-1 (MCP-1) are released attracting monocytes to the area, which become either macrophages or osteoclasts once they exit the blood stream and enter the tissue [23]. The bone-bending theory established by Farrar in 1888 supported the idea that when an orthodontic force is applied to the tooth it is transmitted to all tissues near that force application. Thereby this force bends the bone, PDL, and surrounding tissues in order to induce tooth movement [24]. Moreover, the Biological Electricity Theory proposed in 1962 by Bassett and Becker supports that when the alveolar bone is under force to flex or bend there is a release of electric signals to the surrounding tissues [25]. These changes in electric potential around the bone impact the metabolic processes and result in cellular differentiation, leading to tooth movement. The area with electronegative charge is characterized by elevated level of osteoclastic activity and the area of electropositive charge is characterized by increased levels of osteoblastic activity [26].

An improved understanding of bone remodeling and its role during OTM requires a better understanding of the molecular changes that take place to maintain bone homeostasis. Osteoblasts and osteocytes express RANKL which can bind to its receptor, RANK, on osteoclast precursors [1] [17] [2] [16]. This enables the pathway for osteoclastogenesis which leads to bone resorption. Osteocytes can upregulate or downregulate the expression of RANKL, which in turn impacts osteoclastogenesis [16]. The expression of RANKL is down-regulated by osteoblasts in the presence of TGF β or estrogens [27]. Furthermore, sclerostin, coded by the gene *SOST*, is produced by mature osteocytes, and serves as an antagonist of the Wnt/ β -catenin pathway; sclerostin is able to inhibit osteoblast activity and lead to increase bone resorption [6]. Osteoprotegerin (OPG) is a decoy receptor secreted by osteoblasts, to block differentiation of the

osteoclast precursor cell, which results in bone formation [1]. Therefore, a balance between many regulators and the RANKL/OPG ratio is a critical determinant of bone mass.

Many of these theories were established prior to understanding and further study into the role of osteocytes during OTM. Although it was known that there were osteocytes embedded in the bony matrix, there was a lack of knowledge regarding their role in the overall process. However, the literature now supports a better understanding as to how the osteocyte communicates with surrounding tissues in long bones. Therefore, it is critical for patient care, that scientific research continues to investigate bone biology through OTM and the regulatory factors which can impact tooth movement to make the practice of orthodontics more effective and efficient.

A3: Role of Osteocytes During Orthodontic Tooth Movement

As previously described, there are many theories for OTM that heavily rely on the actions and contributions of osteoblasts and osteoblasts. However, the role of osteocytes during OTM is not fully understood. The most notable function of an osteocyte is its mechanosensing property [5]. It is indeed more than a passive placeholder trapped in a lacuna with no purpose in the bony matrix. This means that osteocytes can detect mechanical stimuli developed from the mechanical loading of bones and communicate with other cells via canaliculi. These channels carry the long, slender cell processes through the bony matrix to allow for signaling molecules to pass and reach other cells [10]. This intricate network of canaliculi develops a web to make indirect communication between cells deeply embedded in the bone matrix possible with cells on the bony surface [28]. Healthy osteocytes are essential for appropriate behavior and performance of bone and other organs. The complex and sophisticated lacuna-canalicular network which is integrated within the bony matrix make up the blueprint for osteocytes to deposit and resorb

bone through a process known as perilacunar/canalicular remodeling [6]. Maintaining mineral homeostasis and bony infrastructure is in large part due to the activity of PLR as a homeostatic mechanism. Moreover, osteocytes have also been found to play a regulatory role between the expression of osteoblasts or osteoclast during bone remodeling [29]. An OTM study with osteocyte-ablated mice reported there was significant decrease in tooth movement since these mice were more resistant to bone loss, which help further define the importance of osteocytes during bone remodeling [7].

During OTM, the force initiated to move the tooth first induces a stage of hypoxia. This is a critical initial step during OTM which signals to the surrounding cells that an event is taking place which requires attention. This change in oxygen levels available to the cells occurs concurrently with load-induced fluid flow changes. The fluid flow dynamics also act as an activator of signaling to the surrounding tissues. In the fluid flow hypothesis, there is a displacement of fluid in the canaliculi of mechanoreceptor cells, the osteocytes in bone, and fibroblasts in PDL, which initiates a response to the strain [30]. The application of force results in a cascade of steps to follow. First, at the site of the orthodontic force where the tooth is loaded with pressure, interstitial fluid is pushed through the canaliculi and around the osteocytes which puts a strain on the cell surface and extracellular matrix [21]. This pressure experienced by the cells starts the reaction to make an environmental change. Cellular activation at the osteocyte through integrins binding results in a release of intracellular molecules that modify gene expression. This stimulation of the osteocyte promotes signaling for differentiation of osteoblasts and osteoclasts to start the bone remodeling process [18] [31]. The fluid-flow shear stress created by the orthodontic force on the tooth to initiate movement is a key player in better understanding

the role of the osteocyte and bone remodeling. Since osteocytes are mechnosensing cells they respond to the changes in the tension and compression of their bony matrix environment.

Stress-induced bone matrix deformation/microcrack formation and changes in fluid-flow shear stress within the system is one of the popular theories that support the role of osteocytes during OTM. When orthodontic force is applied to teeth there is a pressure placed on the alveolar bony matrix and that can be interpreted by the cells as a mechanical load, which was explained previously. This pressure results in a physical change from bone fatigue to actual microdamage on the side of the force. Microcracks are considered one of the first signs of change in the bony matrix after OTM is initiated; they are less prevalent on the tension-side than on the pressure-side of the tooth. Verborgt et. al. reported that during bone remodeling, or bone fatigue, osteocytes undergo the natural death process known as apoptosis. The areas with the highest concentration of osteocytes that underwent apoptosis are regions of the bone with microcracks [32]. The apoptotic bodies released from the apoptotic osteocytes express RANKL which recruit osteoclasts [33]. It was noted that osteoclastic cells were found in the region of the bone fatigue to resorb bone and start the remodeling process [32]. The paper concludes that there is a strong association between microdamage of the bone, osteocyte apoptosis, followed by bone remodeling supported by osteoclasts. This theory supports the idea that osteocyte apoptosis plays an important role in the stimulation or initiation mechanism to signal osteoclasts to target bone resorption after fatigue-induced matrix injury [32].

A4: Understanding the Role of TGF β signaling in bone biology

TGF β is a local regulatory factor that helps maintain bone homeostasis via cellular migration, differentiation, proliferation, matrix synthesis, and apoptosis [34]. This cytokine serves to create a balance between bone formation and bone resorption through physical and

biochemical stimuli. TGF β mediates the crosstalk between osteoclasts and osteoblasts during bone remodeling and supports a healthy bone matrix. With its widespread influence, TGF β also acts on terminally differentiated osteocytes within the bone matrix by inhibiting osteocyte apoptosis, partially through a Smad3 and vitamin D receptor-dependent mechanism [35]. This connection to preventing osteocyte apoptosis, which recruits osteoclastic activity, illustrates the downstream impact TGF β can have on bone remodeling. This powerful cytokine can also reside in the bone matrix in latent form. When osteoclasts begin to resorb bone, latent TGF β ligand is activated through the acidic microenvironment. Once released from the matrix, the active TGF β loops back to signal to osteoblasts for bone formation. Therefore, the presence of TGF β creates a coupled process to maintain balance [36]. The PLR process that occurs by the osteocytes is required during normal conditions for mineral and collagen organization as well as after fatigue injury like OTM. Simpson et. al. reported TGF β plays a molecular role for the stability and survival of osteocytes from cancellous bone in a long-term culture in an *ex vivo* loading bioreactor [37]. Understanding this dynamic between osteocytes and TGF β during PLR provides more insight into how bone quality may be impacted by changes in TGF β availability.

The work by Dr. Alliston's team highlights the relationship between osteocyte-intrinsic PLR and TGF β as a regulatory factor in long bones [11]. They showed that TGF β signaling controls bone quality and osteocytic PLR via repression of several key genes using a mouse model with deletion of TGF β receptor I. Furthermore, this group also examined effect of TGF β on MLO-Y4 osteocyte-like cells and OCY454 osteocytes *in vitro*; their conclusions reinforced the likelihood that TGF β stimulates PLR in an osteocyte-intrinsic manner. Therefore, when there is direct inhibition of TGF β signaling due to deletion of the TGF β receptor II, there is an effect on the osteocyte-intrinsic PLR process which ultimately affects bone quality. Specifically, the

length of the canalicular projections in the using DMP1-Cre mice, resulting in $T\beta RII^{ocycy-/-}$ bone showed a reduction of 50% compared to the WT mice. Also, the canalicular network was retracted and visibly rounded relative to the WT samples. These findings also showed that there was an even greater impact on PLR gene expression with deletion of $T\beta RII$ compared to their previous study of $T\beta RI$ ablation. These changes to the PLR communication and inability to regulate bone homeostasis leads to an increase in trabecular bone mass due to the lack of bone resorption. There was no change in cortical bone mass and thickness. They concluded through a fracture toughness test that $TGF\beta$ regulates bone quality in an osteocyte-intrinsic manner, specifically through extrinsic toughening mechanisms that limit crack growth when the bone is under stress or fatigue [11].

Disrupting $TGF\beta$ signaling has a profound impact on the bone quality and studying this pathway and interacting effectors further can help uncover more therapeutic targets to recalibrate bone homeostasis, such as after OTM is completed. Thus, understanding how $TGF\beta$ regulates alveolar bone quality in an osteocyte-intrinsic manner can open doors to new treatment.

The purpose of the proposed experiments was to increase our understanding of the molecular mechanisms involved in bone remodeling induced by orthodontic forces. Establishing the role of osteocyte $TGF\beta$ signaling in OTM may help in the development of new, innovative approaches to control tooth movement outcomes.

B: Materials and Methods

B1: Background

This study aimed to investigate the impact of defective $TGF\beta$ signaling in osteocytes on the alveolar bone remodeling process and its direct correlation to OTM. Male and female $Dmp1-$

Cre^{+/-}; TβRII^{fl/fl} and Dmp1-Cre^{-/-}; TβRII^{fl/fl} littermate controls underwent general anesthesia and were subjected to single-sided orthodontic treatment in the right left quadrant. Untreated mice that did not undergo OTM were used for the control group. In the experimental group, the maxillary left side had an orthodontic NiTi spring ligated and bonded from the first molar to both maxillary incisors. Treatment lasted 14 days, a time frame previously established to be effective in studying OTM [38]. A widely utilized mouse OTM model was mirrored for this study [39] [7] [9] [38], however, OTM has never been performed in TβRII^{ocy}^{-/-} mice. At the completion of the study the mice were humanely euthanized as per IACUC protocols, and tissue samples were harvested for further analysis. OTM can be studied in many different animal species, but mice were chosen due to their natural dentition landscape. Mice have one maxillary incisor in each quadrant and 3 molars separated by a long span or diastema (approximately 7mm) This natural distribution of teeth and edentulous space allows for OTM to be mimicked as it would be in a human moving teeth in the mesial/distal direction.

B2: Funding

Funding for this project was provided by the American Association of Orthodontics Foundation and the National Institutes of Health (NIH) under the leadership of Dr. Christine Hong.

B3: Sample Size

A power analysis was performed using conservative assumptions and based on data from prior studies by our group and others. We used the mean and standard deviation according to the type of assay from previous studies as well as previously performed OTM studies for the power calculation. Most OTM studies performed on mice required a sample size of n = 6-9 to detect

significant differences in the craniofacial skeleton [11] [39] [40]. For OTM *in vivo* studies, power analysis using G*Power 3.1 shows >80% probability in detecting a difference between genotypes and sex with a two-sided alpha level of 0.05 and a sample size of 9 mice, yielding an effect size of $d_z=1.3$. Using fewer animals does not allow us to detect a difference that would be clinically relevant, which we discuss later in this thesis.

B4: Subjects

A transgenic mouse line with osteocyte-specific deletion of TGF β receptor II (TBR II) was used for our experimental group. 12-week-old male and female $Dmp1-Cre^{+/-}; T\beta RII^{fl/fl}$ ($T\beta RII^{ocyc^{-/-}}$ mice) and $Dmp1-Cre^{-/-}; T\beta RII^{fl/fl}$ littermate controls (CTRL) were divided into four groups: Control (CTRL) and Experimental (OTM) including both cre- controls and cre+ mutant mice for each sex. Control groups did not undergo OTM but underwent the same sedation and received the same post-surgical soft gel diets. The OTM group had an orthodontic appliance applied to the maxillary left side only. All mice were euthanized at 14 days with CO₂ asphyxiation and their maxillae were harvested, hemisected, and fixed in 10% buffered formalin for MicroCT analysis. The protocol was approved by the University of California, San Francisco Animal Research Committee.

B5: Sedation and Pain Control

Prior to surgery and orthodontic appliance placement, mice were anesthetized by intraperitoneal injection of ketamine (87mg/kg) and xylazine (13mg/kg). 200uL Ketamine (100mg/mL) + 160uL Xylazine (20mg/mL) + 640 uL Saline = 1 mL stored at 4C. 120-150 uL of the 1 mL was used for IP injection per mouse (for adult mice 20g, anesthetized for 1.5-2 hours).

Although the procedure was non-invasive and bleeding was minimal, the mice were also administered SR Buprenorphine (1.3 mg/mL) injected pre-operatively IP for analgesia.

B6: Orthodontic Appliance Treatment

The mouse maxilla consists of two central incisors and three molars on the right and left sides. Since mice have maxillary incisors with long and curved roots, these teeth were able to serve as absolute anchorage units for this experimental set up.

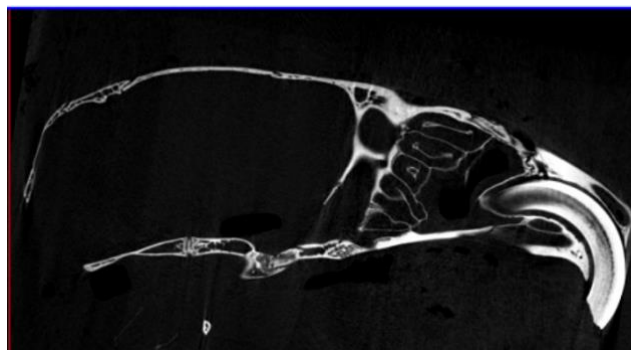


Figure 1: This sagittal cross-section of MicroCT data of 12 week control mouse skull illustrates the robust nature of the maxillary incisor tooth root. The crown to root ratio for the incisors is favorable to induce OTM.

To minimize the movement of the maxillary left incisor, it was joined with the right incisor with bonding resin material [38]. Since there is a natural anatomic space between the incisors and posterior molars, these teeth made an ideal set up to mimic OTM through an edentulous space by moving the maxillary first molar mesially. A key factor to consider in this OTM mouse model is the placement of the appliance on the incisors since they will continuously erupt. Due to this anatomic feature, the appliances were checked for the first 5 days after surgery and then every third day to ensure the incisors were not interfering with the appliance. If any interferences were present, the lower incisors were trimmed 1-2 mm using a ligature cutter.

The orthodontic appliance used in this study was designed to protract the maxillary first molar mesially with a 3–5 gram light force [41]. The NiTi closed-coil spring (Ultimate Wireforms,

Bristol, Connecticut, USA) was attached to the first molar and both central incisors using a thin .008 inch stainless steel ligature wire (Ultimate Wireforms, Bristol, Connecticut, USA)

[42](Figure 2).

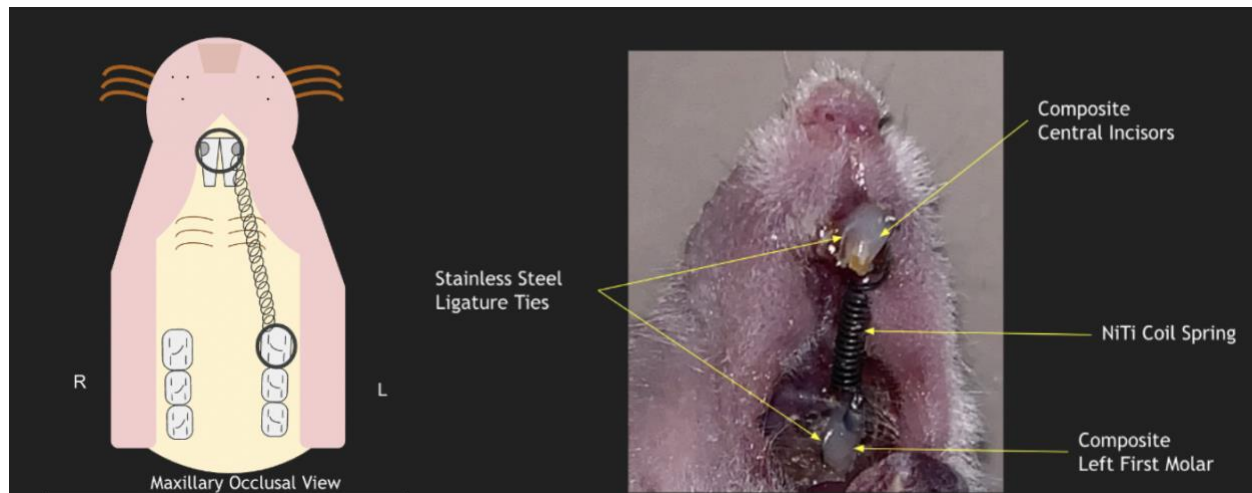


Figure 2: Schematic on the right and in-vivo on the left of the orthodontic appliance with all the components: ligature ties, coil spring, composite, and bonding material.

The mouse maxillary first molar has a natural undercut on its distal interproximal surface, which helped to maintain appliance securely under the contact. Also, a retention groove was made using a high-speed handpiece on the incisors distal proximal surface about .5mm from the gingival margins at a depth of .5mm to help secure the anterior ligature wire, highlight by two dark gray half-circles in Figure 2. Additional stability was achieved by adding the bis-GMA composite resin after self-etching primer (Transbond Plus, 3M Unitek, Monrovia, CA) and light cured into the retention grooves of the anterior teeth and the mesial-lingual surface of the maxillary first molar to secure the wire.

B7: MicroCT Protocol

Animals in all groups underwent *ex vivo* MicroCT imaging at Day 14 after euthanasia. Imaging was performed at the UCLA Core Center for Musculoskeletal Biology and Medicine (CCMBM) MicroCT core using Scanco VivaCT40 (Scanco Medical, Bruttisellen, Switzerland)

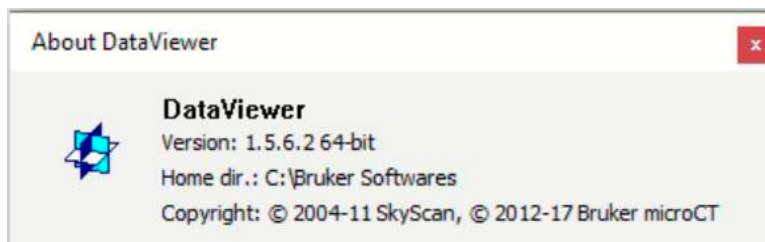
for animal imaging as previously performed by our group and Scanco MicroCT50 (Scanco Medical, Bruttisellen, Switzerland) for specimen imaging [43]. The non-experimental mouse groups with no OTM were also scanned to control for potential effects of radiation on bone homeostasis and quality. For *ex vivo* scanning, the heads were scanned at an image resolution of 10 μm distance with 60kV using a 166- μA x-ray source and a 0.5mm aluminum filter, 0.3 degree rotation per seconds. To ensure scan consistency, a calibration phantom of known geometry (a dense cylinder) was included for each scan.

B8: MicroCT Protocol and Analysis

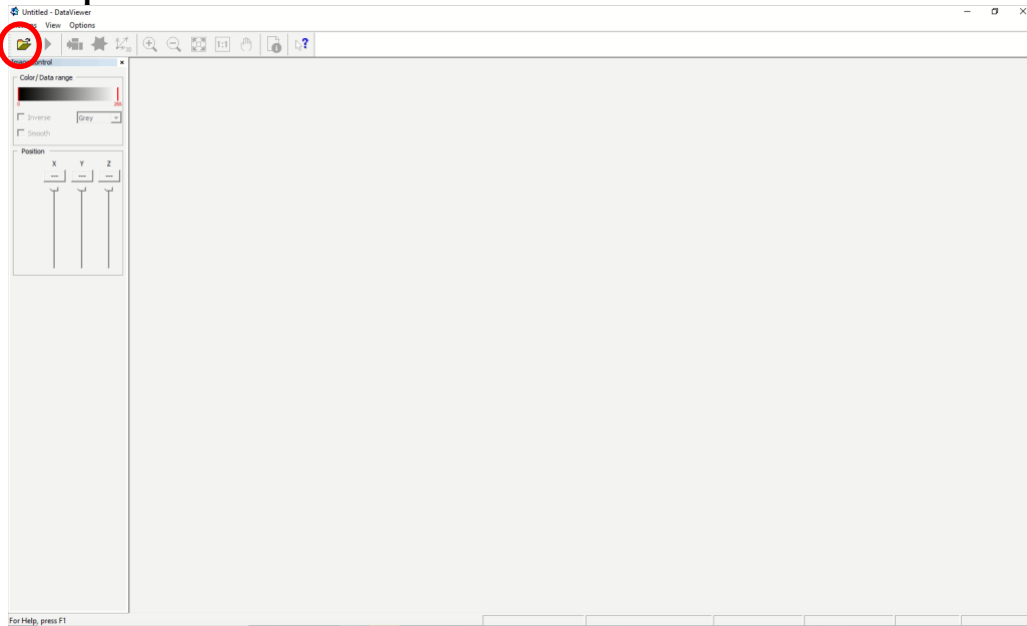
After scanning the mice skulls and acquisition of the MicroCT data files, the images were reoriented on each 3-dimensional plane using Bruker Software DataViewer V1.5.6.2 to align the palate parallel to the transaxial plane. We established a step-by-step protocol for each parameter of analysis:

B8.a: Orientation

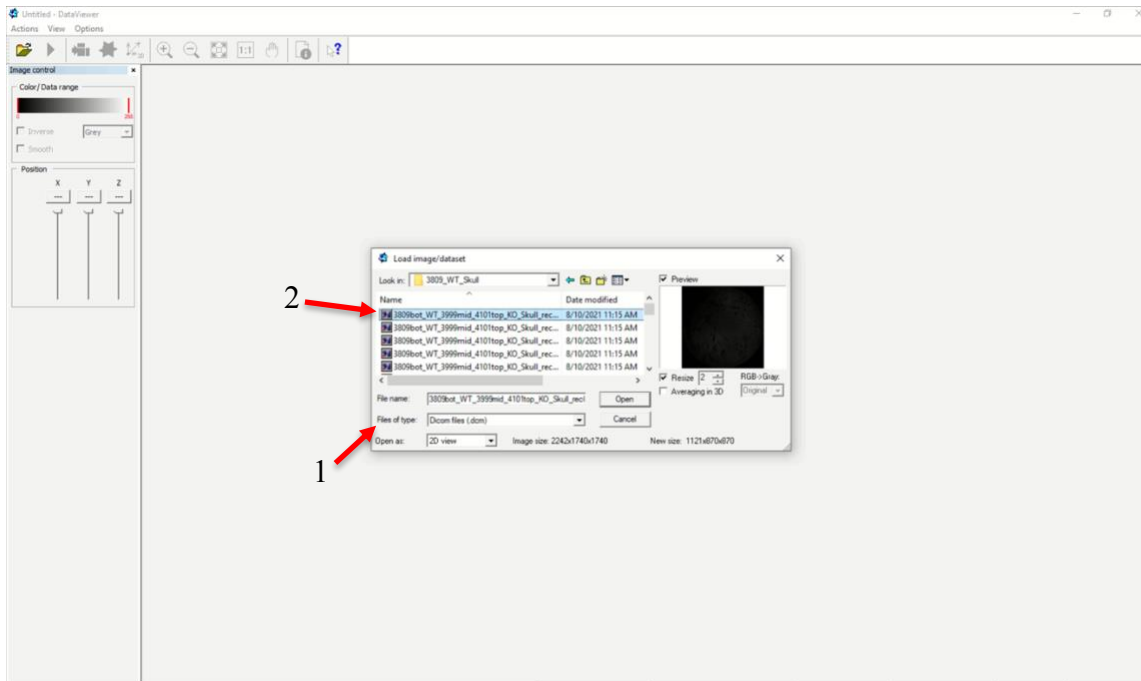
1. Obtain the Bruker Software DataViewer V1.5.6.2 and save the software the C:/ of the desktop.



2. Select Open Dataset.



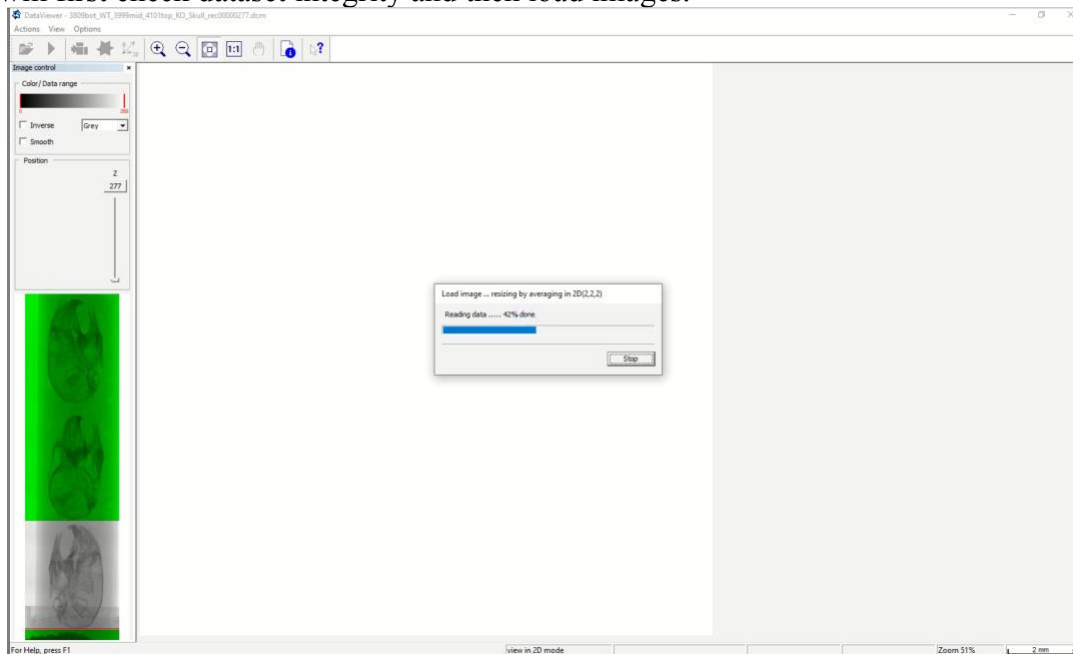
3. Open the folder for the scanned sample and select file types to view: **Dicom files (.dcm)**, then step two - double click on one image. DataViewer will automatically load all the pictures in its program.



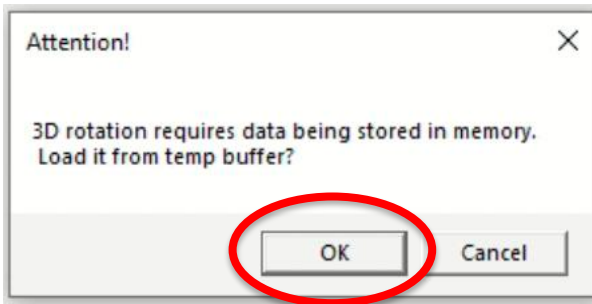
4. Click on Load for 3D Viewing



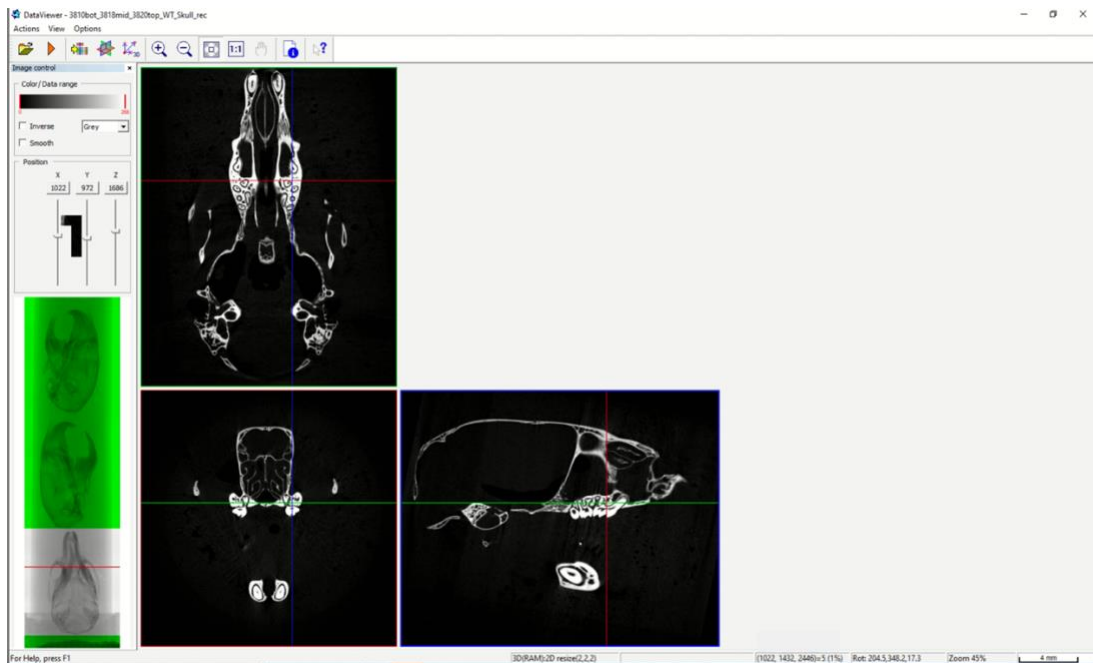
5. It will first check dataset integrity and then load images.



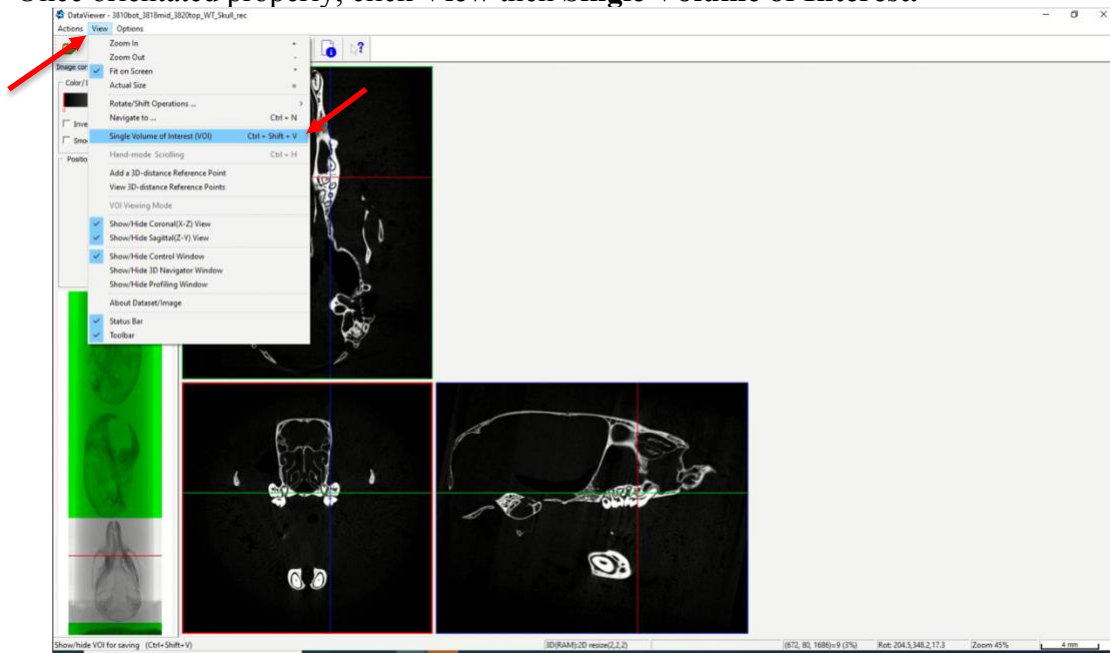
- Right-click on mouse and control on the keyboard to manipulate the imaging in all three planes of space: level occlusal plane of molars horizontally, level palatal suture vertically, and align all three planes of space to be perpendicular to each other. Press OK for “Attention!” popup.



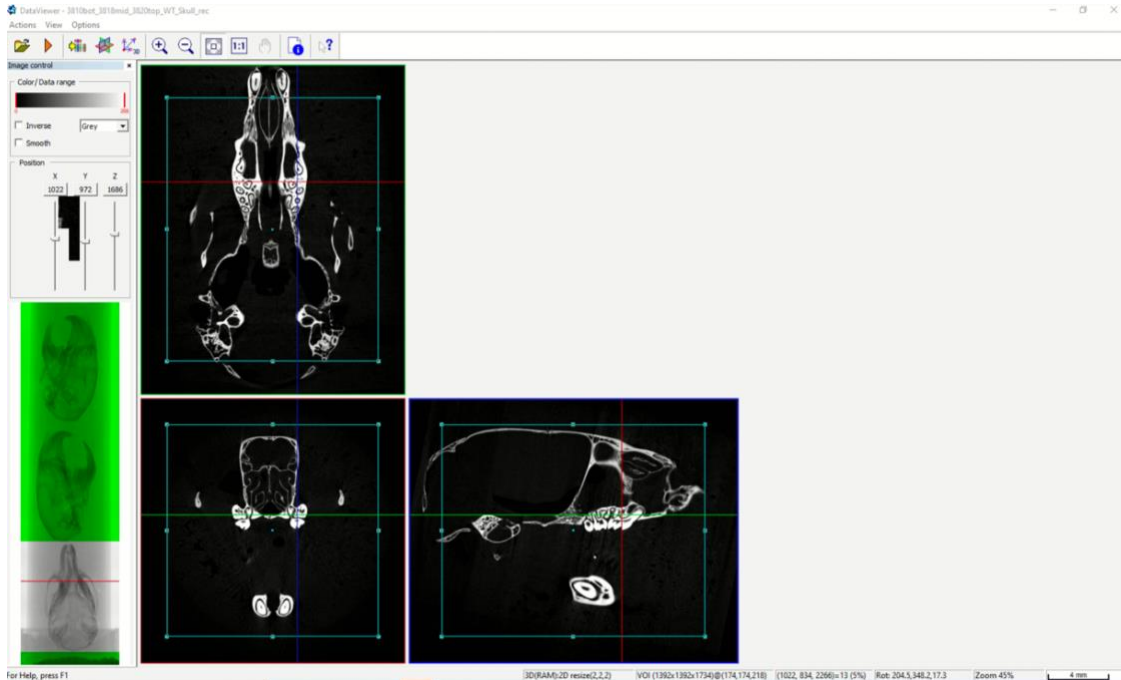
- Complete orientation in all three planes of space.



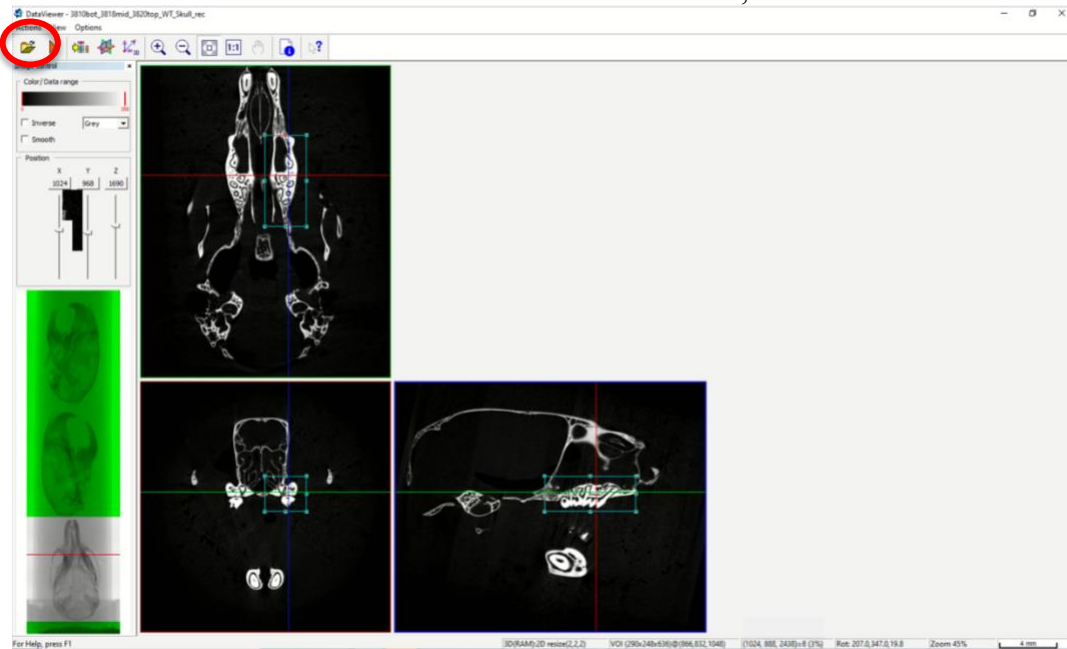
8. Once orientated properly, click **View** then **Single Volume of Interest**.



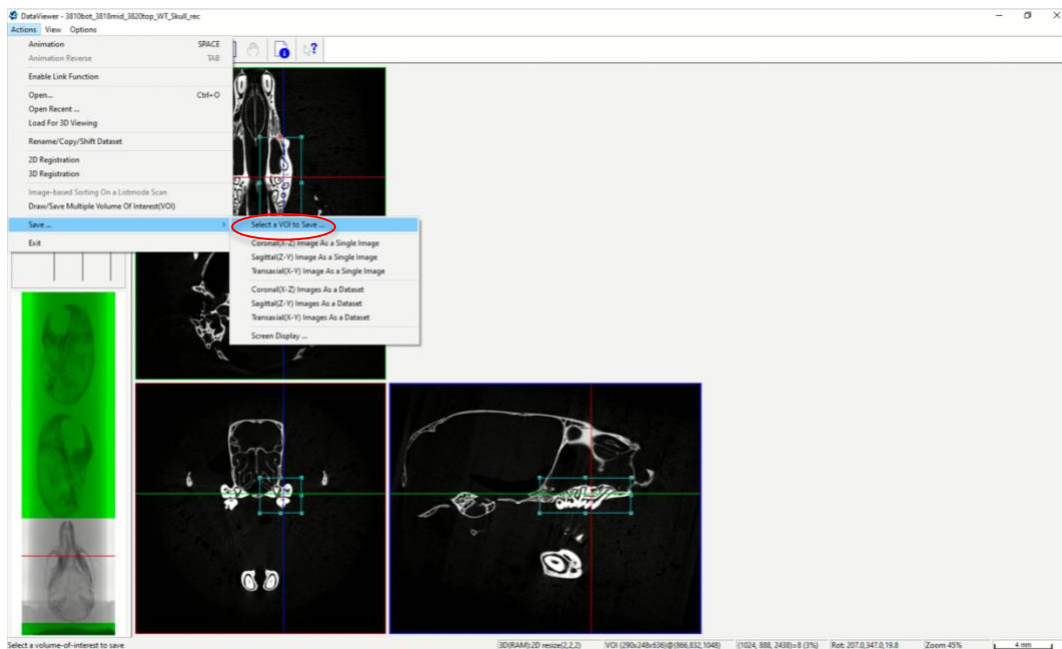
9. Manipulate the blue box that appears with right click on the mouse at the corners of the box to highlight the region of interest: maxillary left molars.



10. Once the selection for the volume of interest is done, click **Actions**.

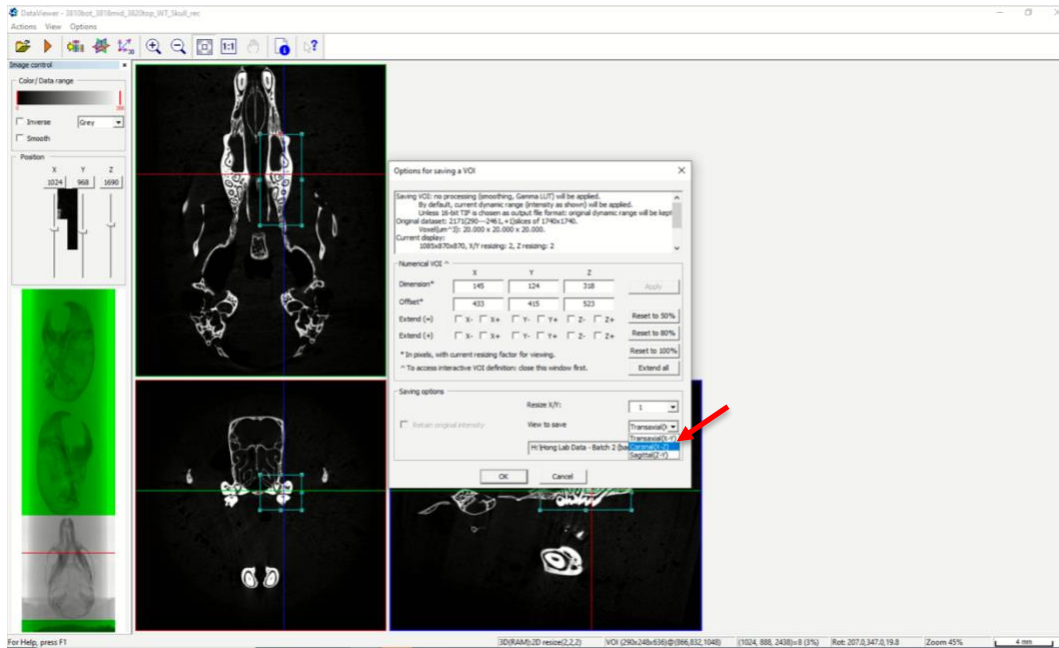


11. Click **Save...** and then **Select a VIO to Save...**

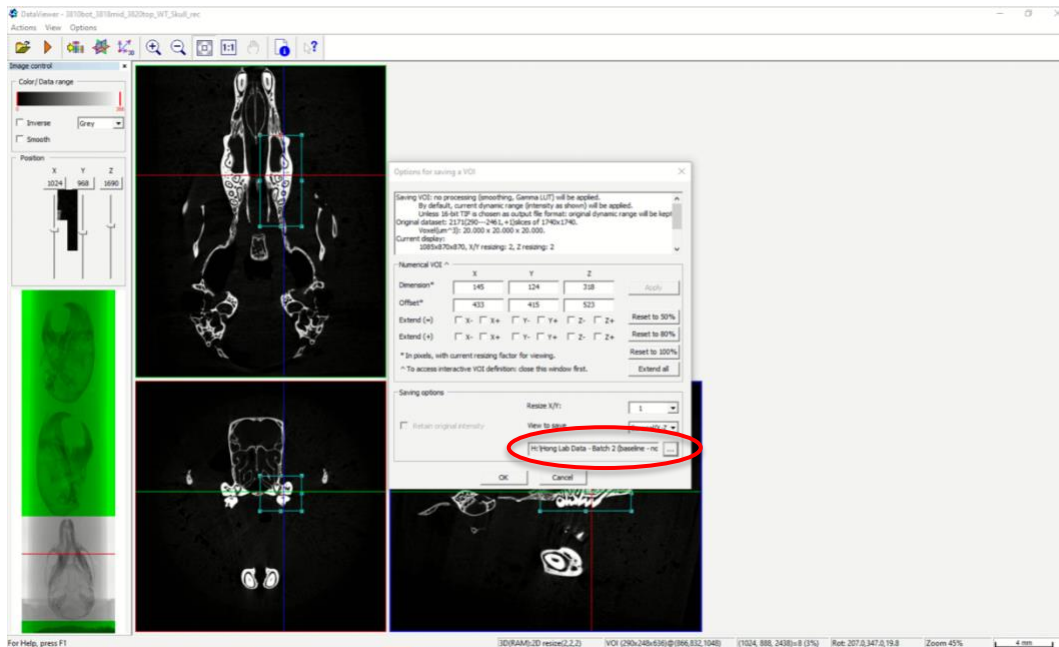


12. Pop-up dialogue “Options for saving a VOI” will appear. Select view to save:

Coronal (X-Z).



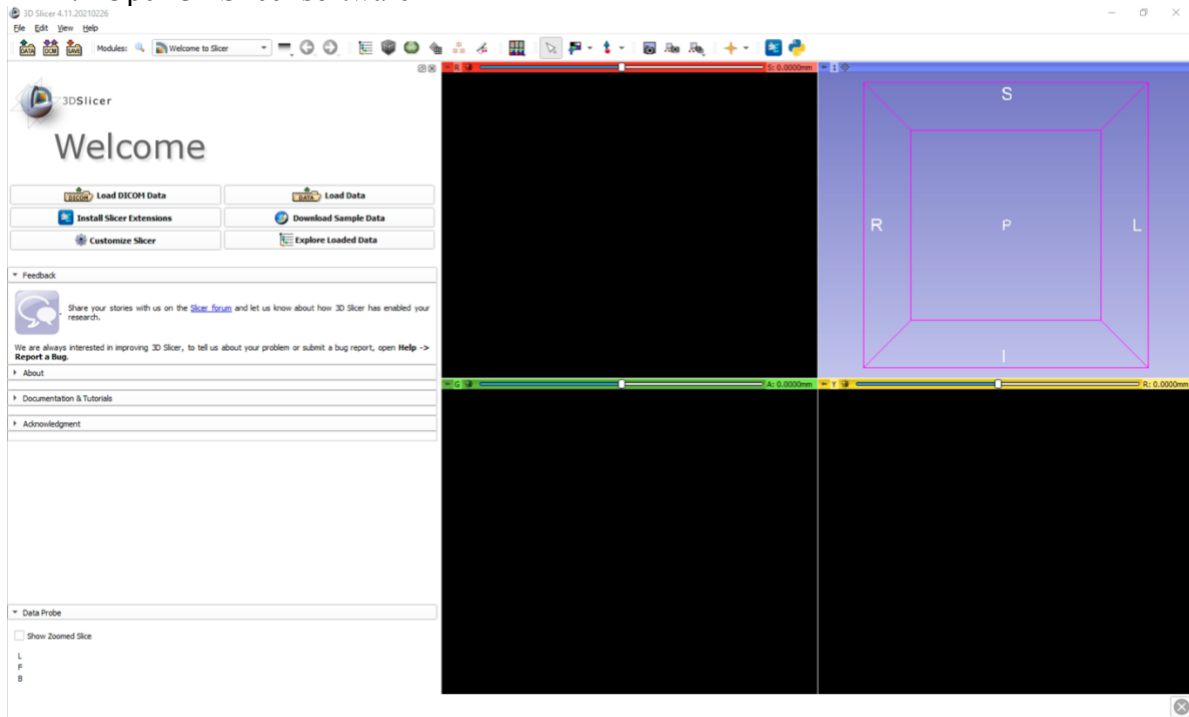
13. Select a destination folder for the new “region of interest” file to be saved by clicking “...”.



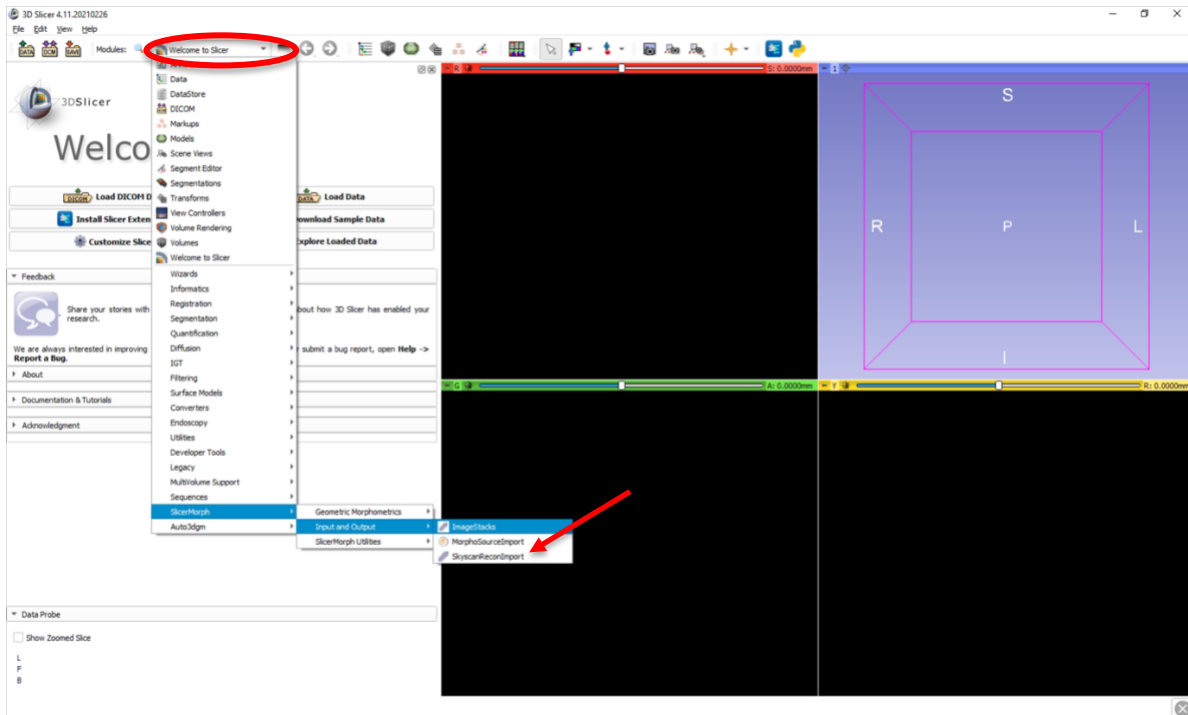
14. Now that the file is saved in the coronal view it can be opened in the 3D-Slicer software in order to analyze the linear tooth movement distance between the molars; it can also be opened in CTAn for volumetric analysis.

B8.b: Linear Distance of Orthodontic Tooth Movement

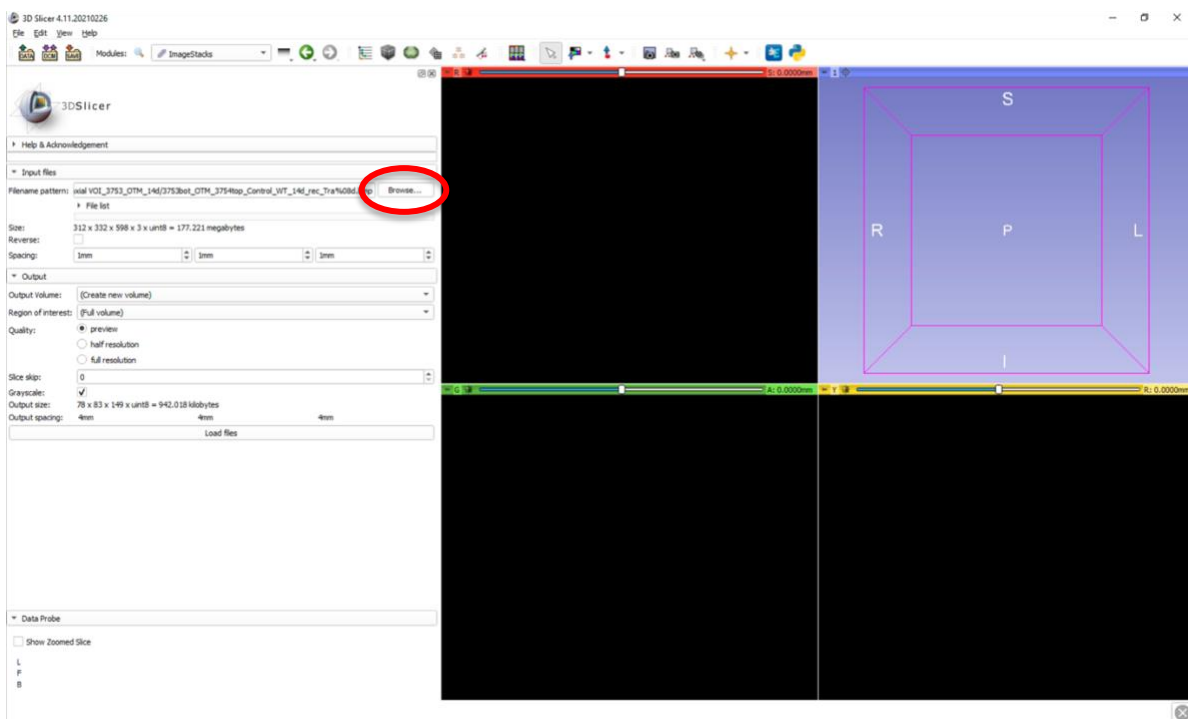
1. Open 3DSlicer software



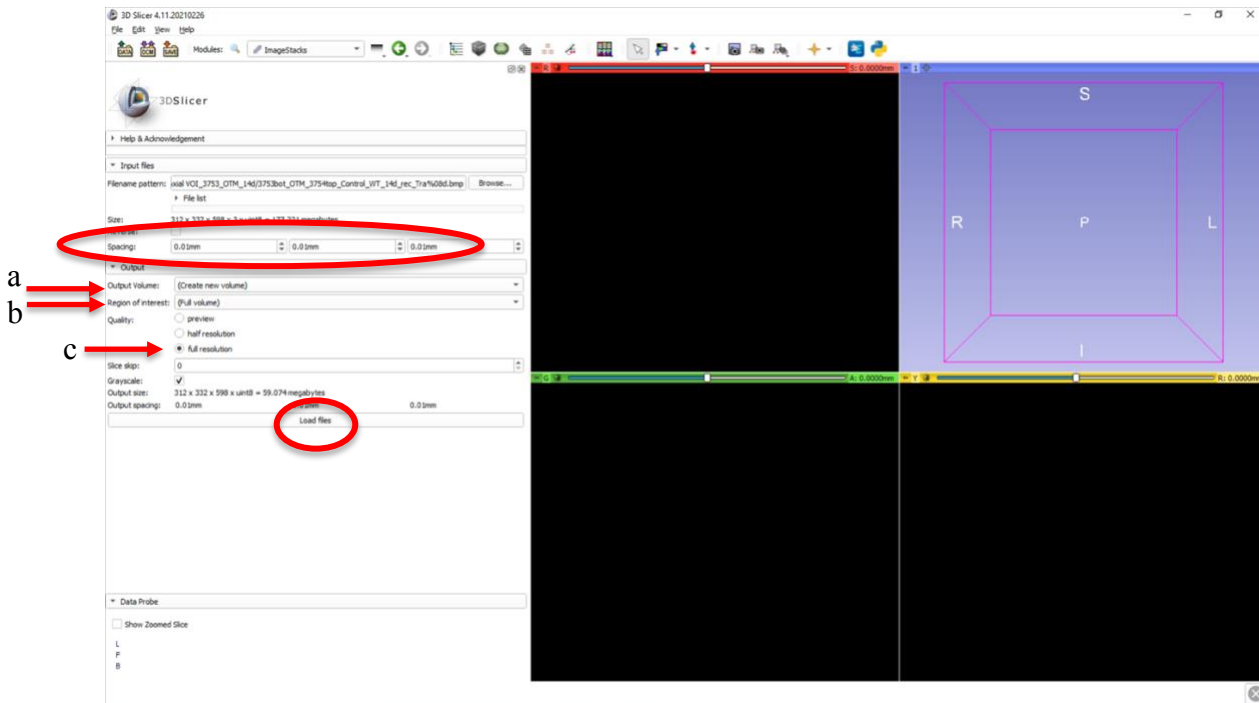
2. Select the drop down menu → SlicerMorph → Input and Output → ImageStacks



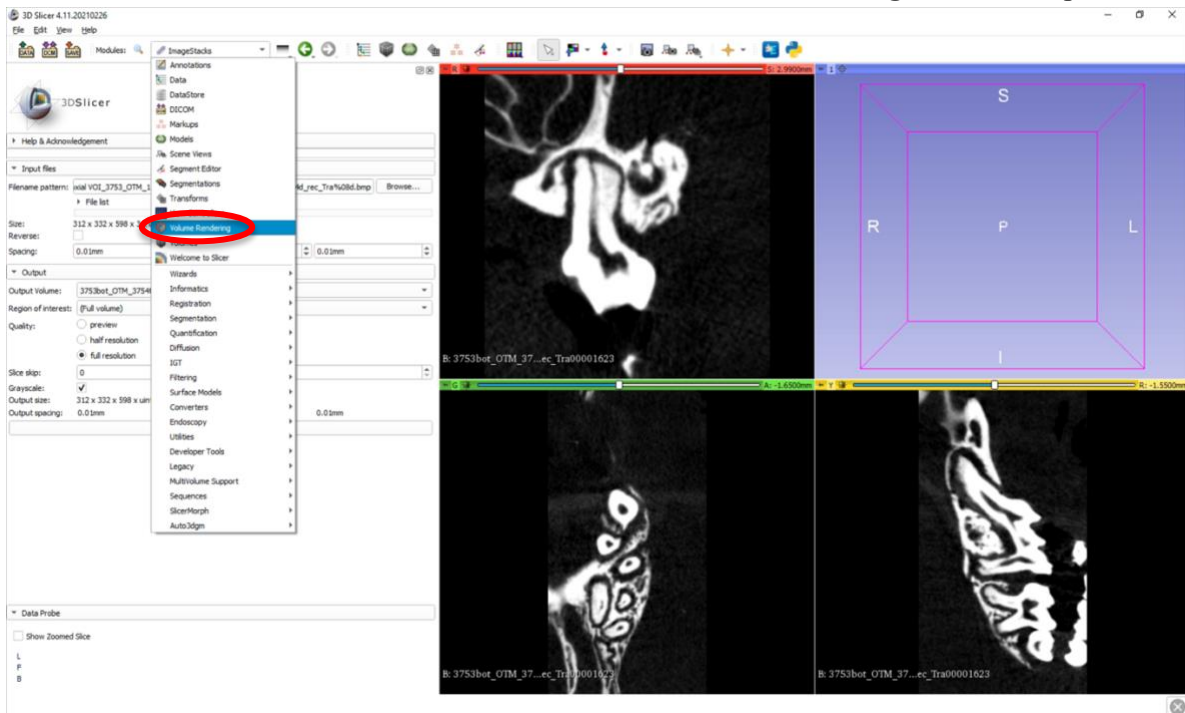
3. Select **Browse...** and double click on one file in the folder of interest



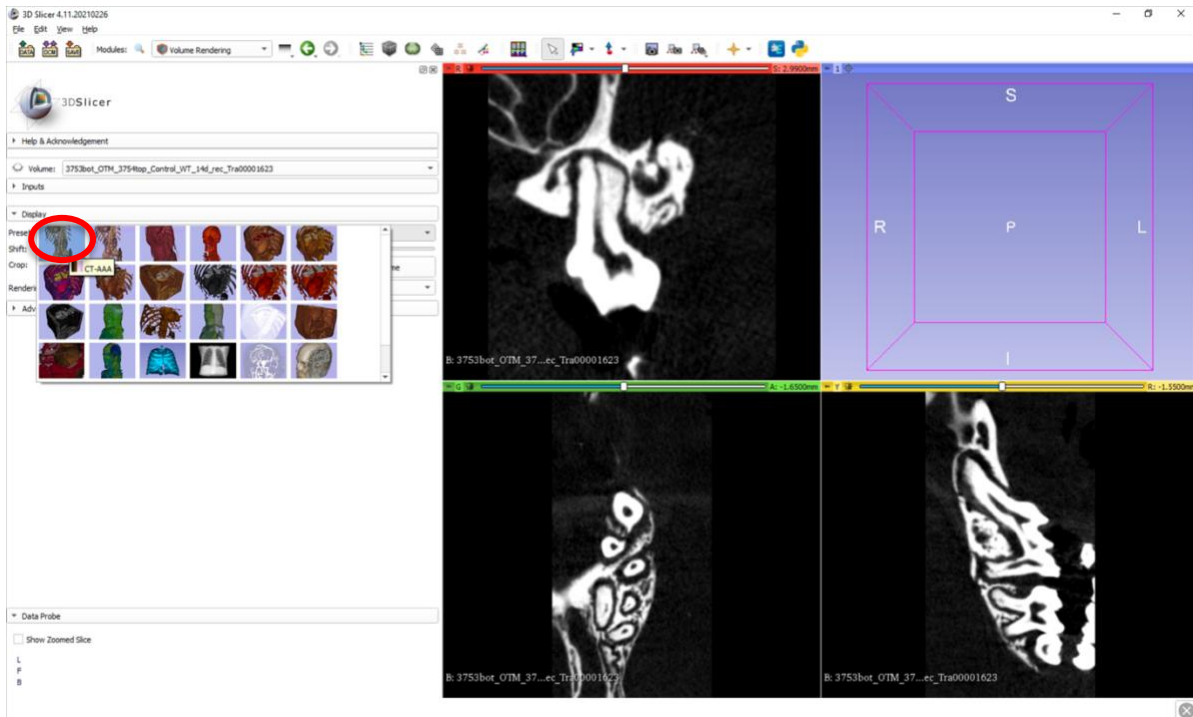
4. Change the spacing numbers to **0.01mm** in all three planes of space.
 - a. Output Volume: (Create new volume)
 - b. Region of interest: (Full volume)
 - c. Quality: full resolution



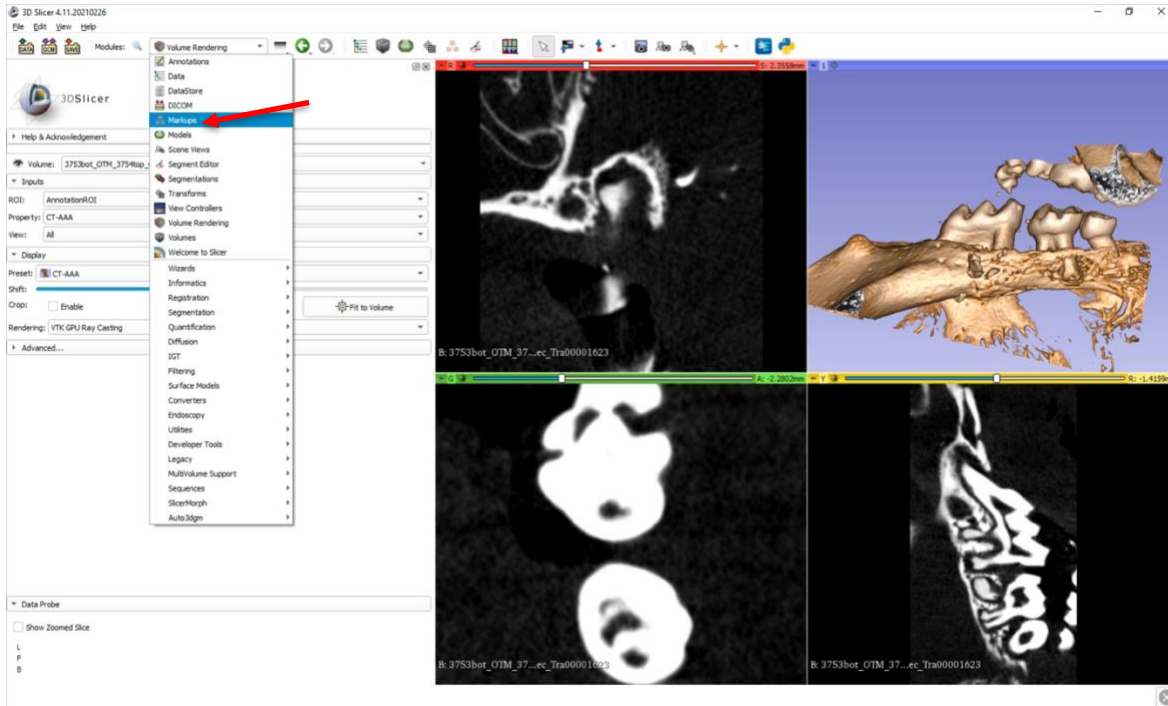
5. Once the microCT file deck is loaded, select **Volume Rendering** from the dropdown menu



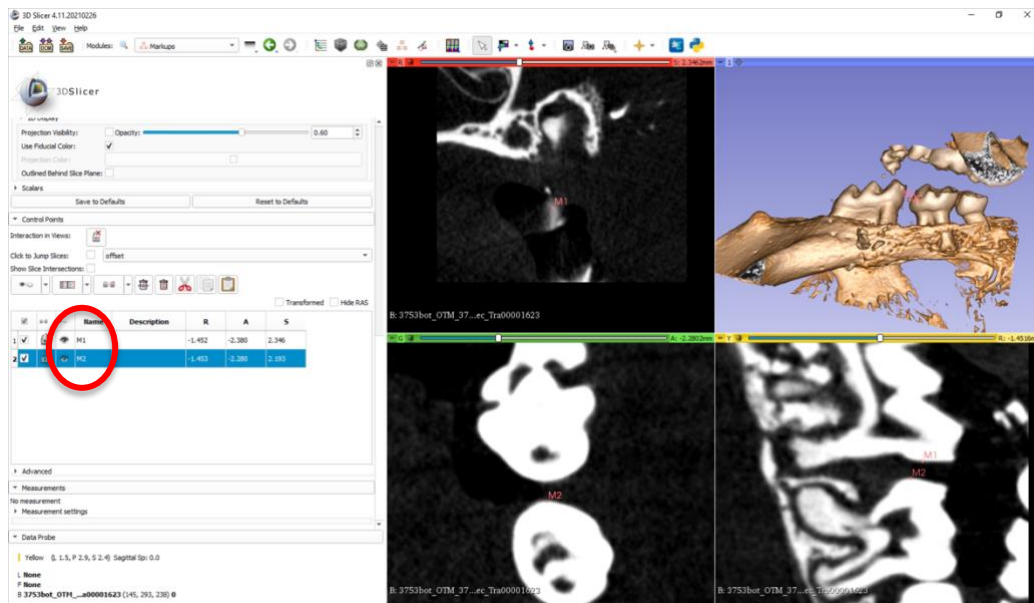
6. In the Display section, select preset: CT-AAA



- In the upper right box, the volume rendering will appear. Zoom in on the image until it is large enough to visualize clearly. Then, select **Markups**. Select this caption twice to create two markup points, one for each molar of interest.



- Left click on the mouse to rename the points **M1** and **M2**, which will represent the points for height of contour on the first molar and second molar.

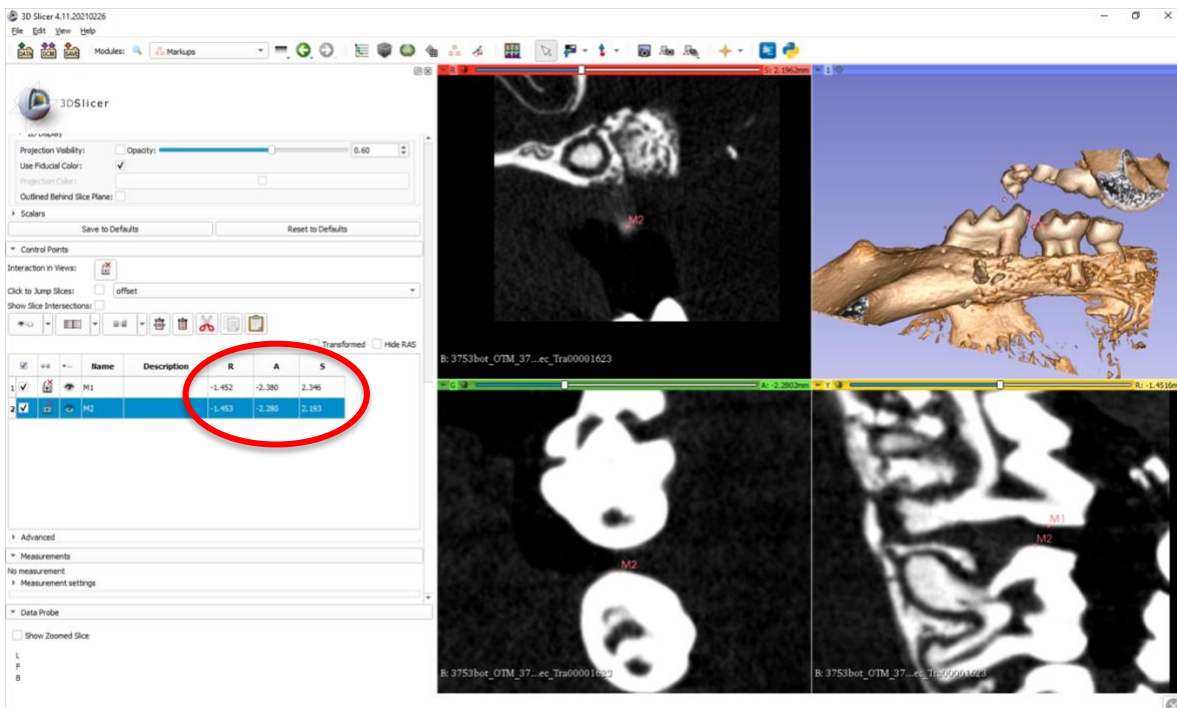


9. Use the scroll bars to move through the slices of the microCT in all three planes of space to find the height of contour on the first molar and second molar. Once located put the marker at that point desired. Record your points in a separate excel sheet to calculate the OTM distance as follows:

- Summed linear distance: highlight both point M1 and M2, right click, summed linear distance measure = **c value**
- Subtract the “**s value**” for M1 from the “**s value**” for M2 = **a value**
- In excel calculate: **b value** = $\text{SQRT}((c^2) - (a^2))$

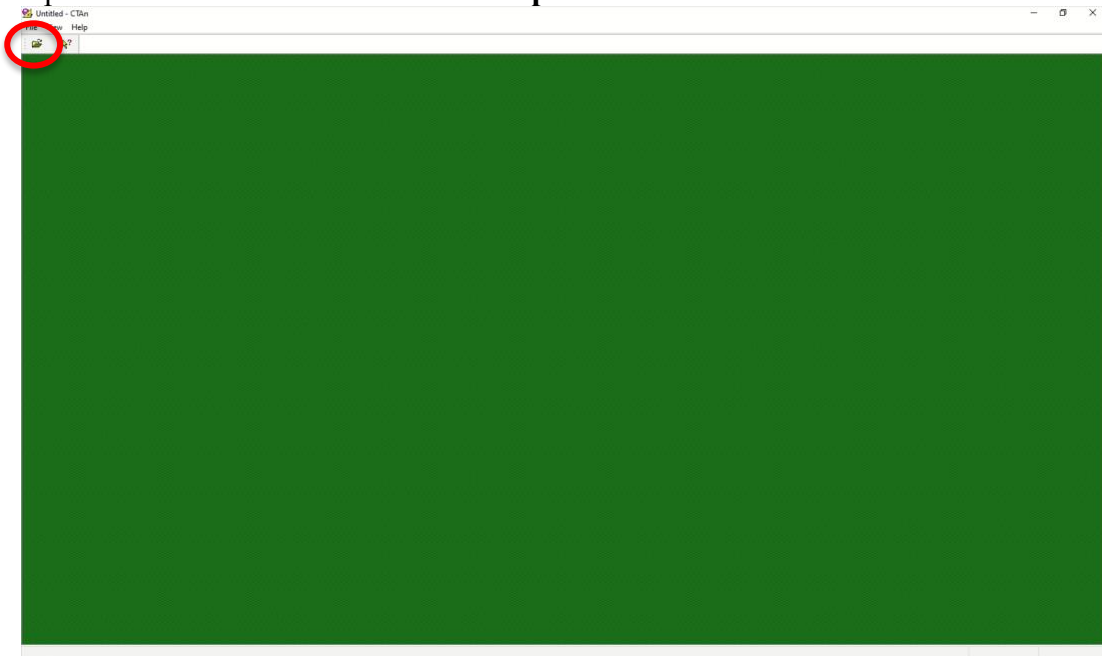
- Excel:

M1 to M2 distance (c value) (mm) (summed linear distance)	(a value) difference in s plane of space (mm)	b value (mm)
--	--	---------------------
- b value** * 1000 = *distance of linear OTM in um*



B8.c: Volumetric Measurements

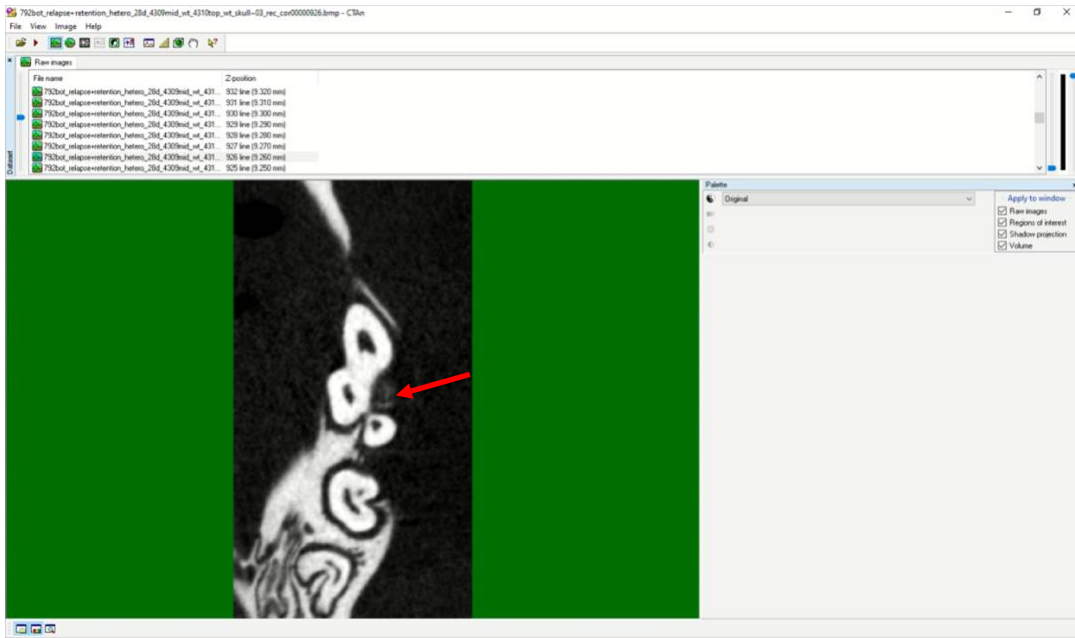
1. Open the CTAn software and click on **open file**.



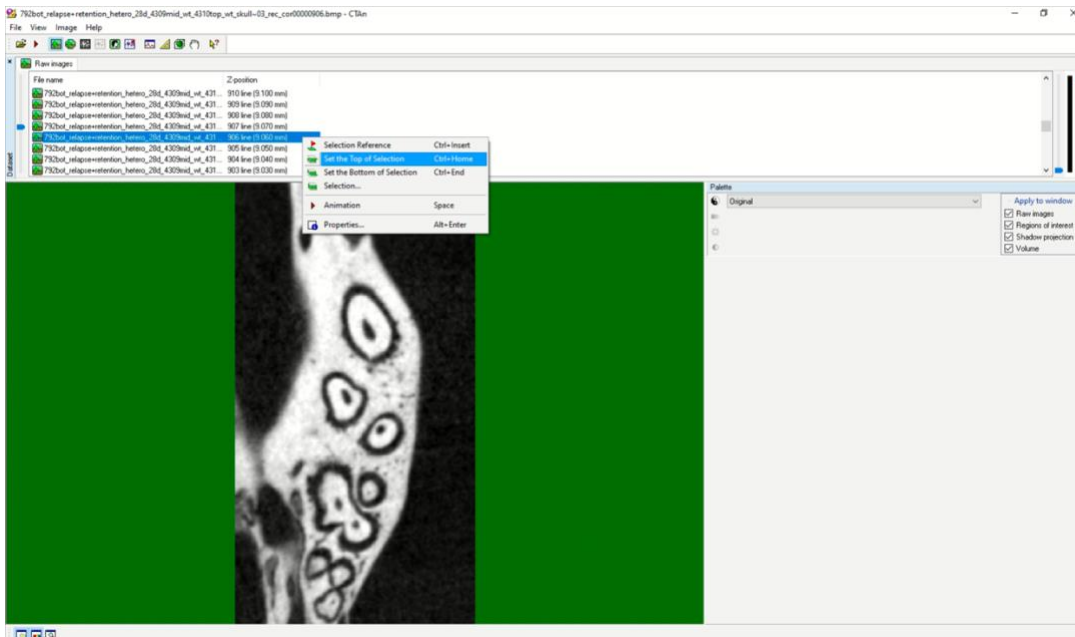
2. Find the file of interest and double click on the file to load. Select **open**.



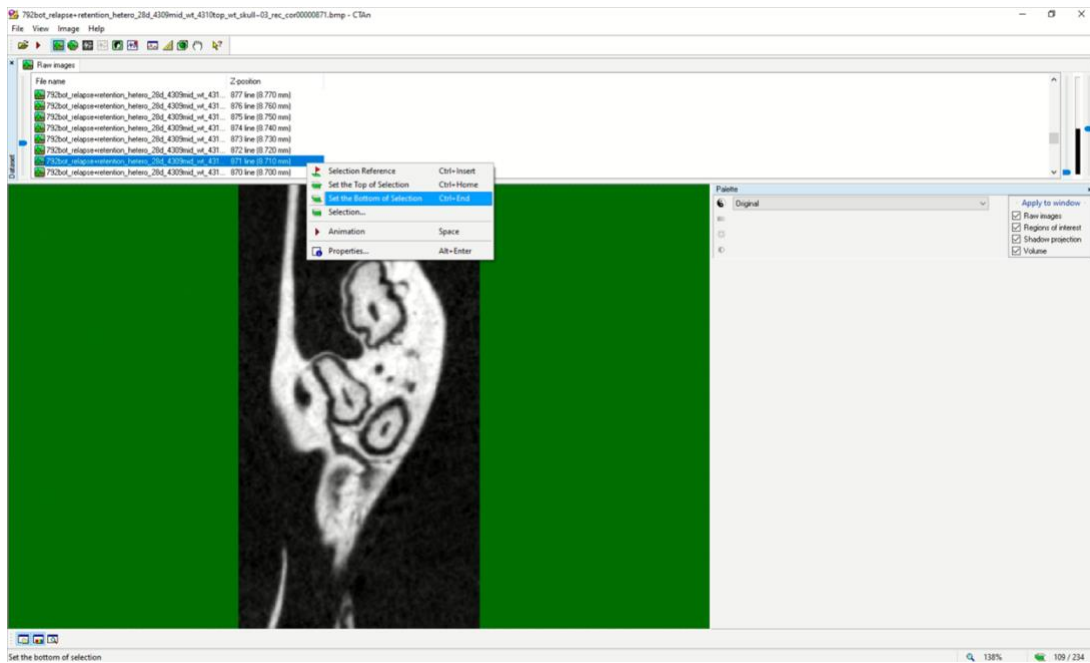
3. Scroll through the files and find the slice that shows the first speck of bone for the furcation area.



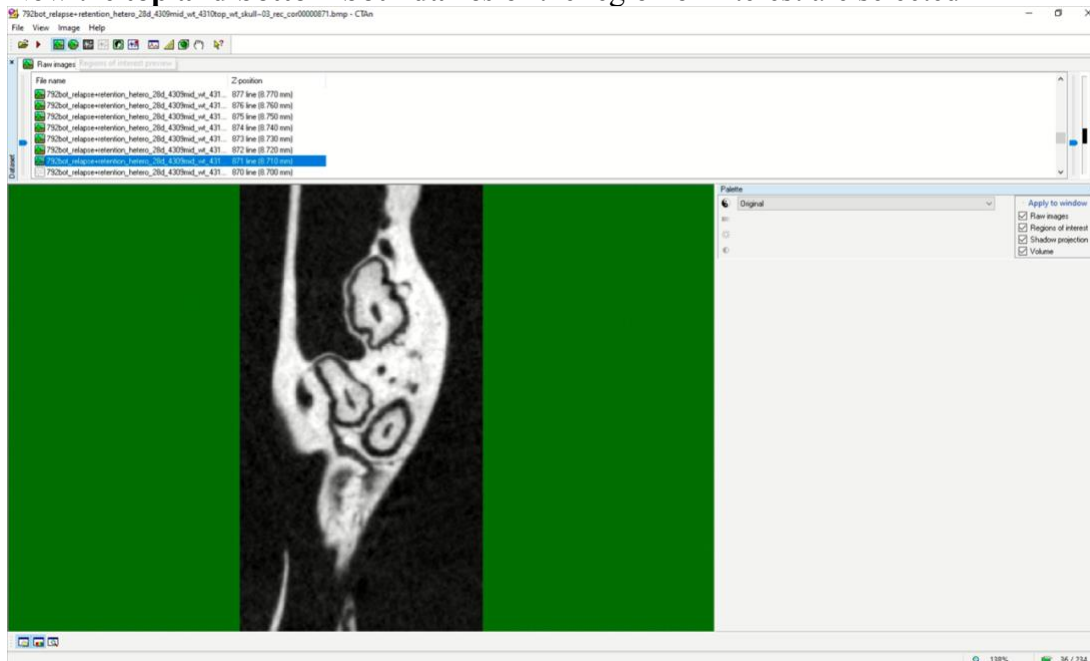
4. Use the file Z position and subtract **0.2mm** to find the first slice for the region of interest.
Right click on that slice and select **Set the Top of Selection**



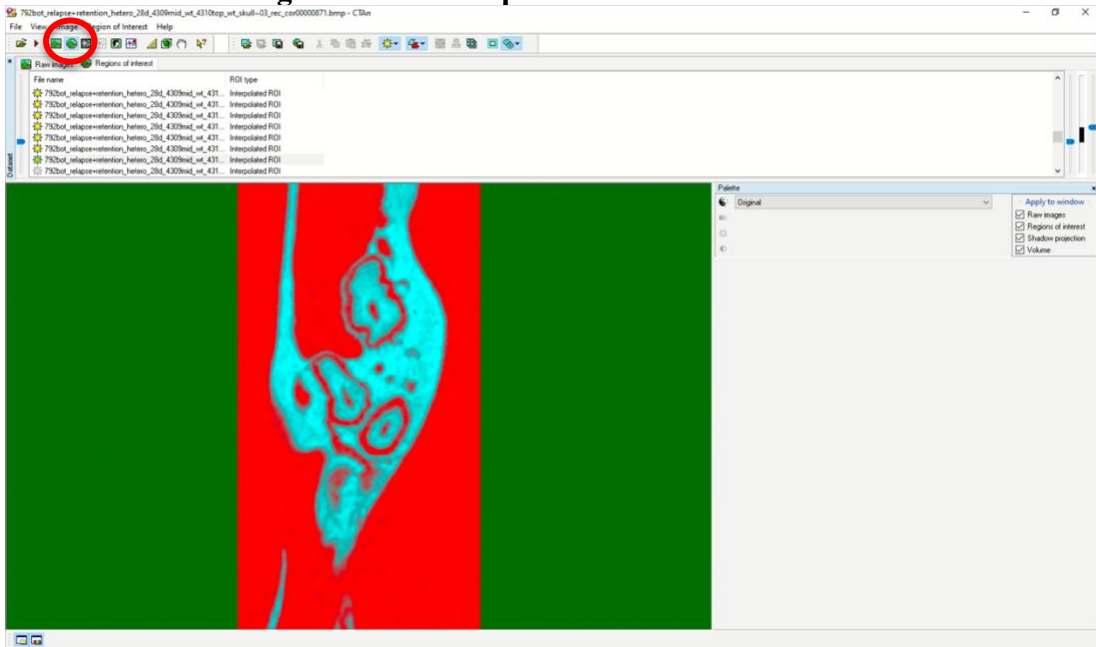
- From the **Top of Selection** and subtract **0.35mm** to find the slice for the region of interest. Right click on that slice and select **Set the Bottom of Selection**



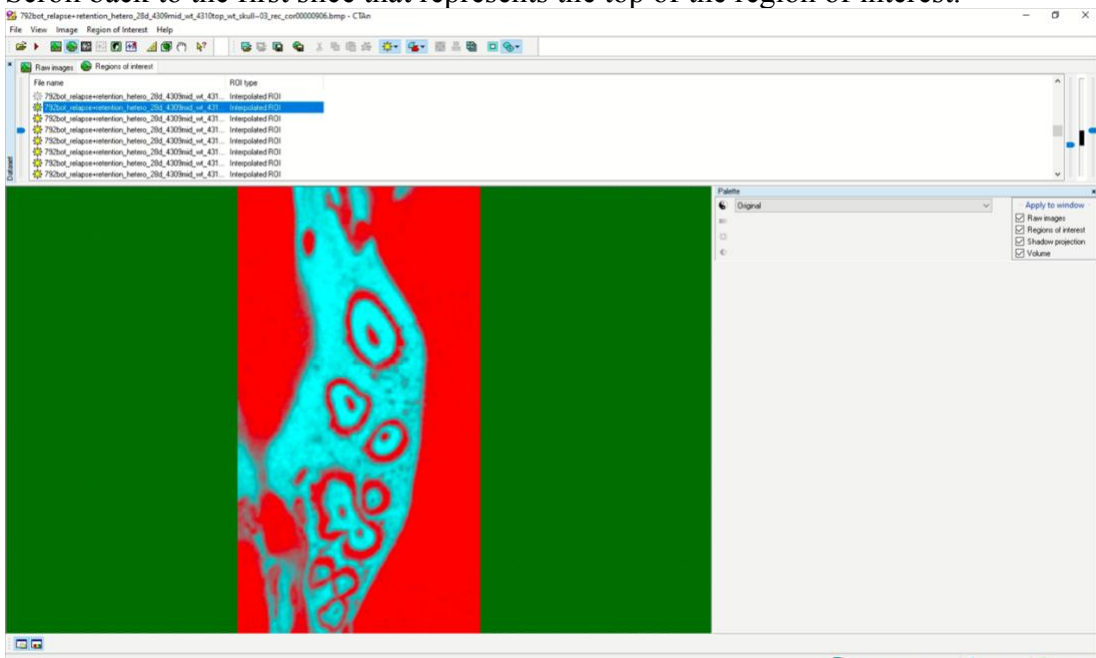
- Now the **top and bottom boundaries** of the region of interest are selected



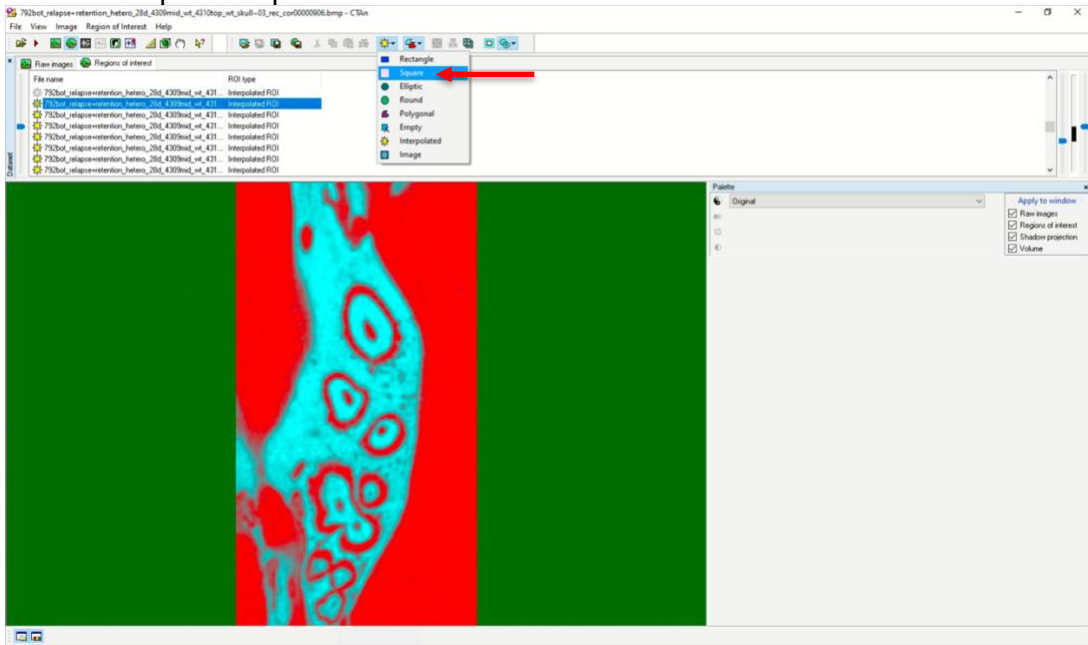
7. Select the next tab **regions of interest preview**



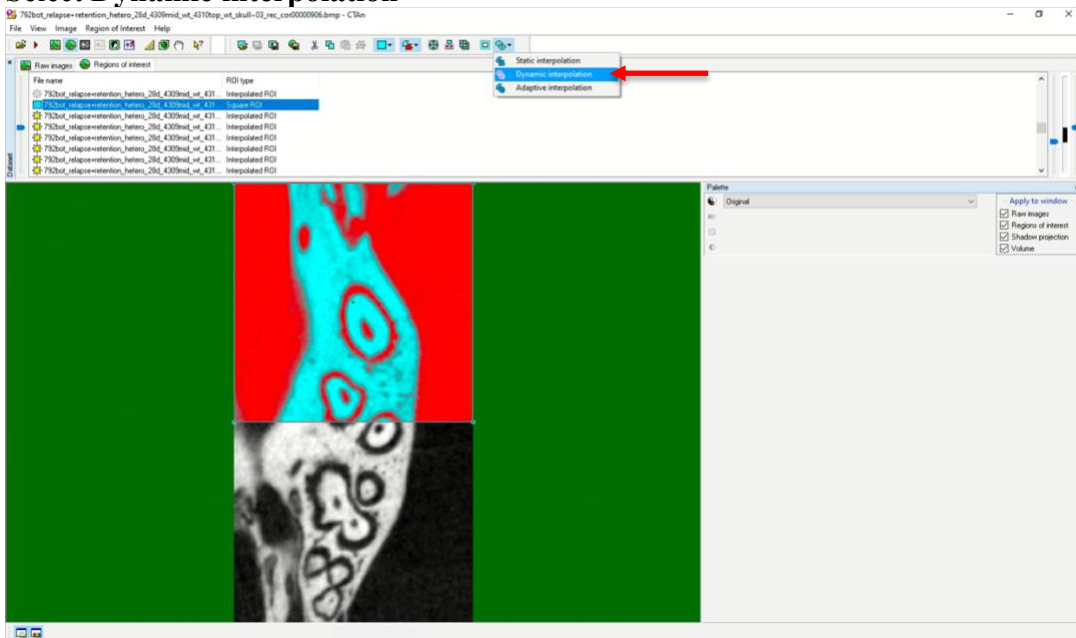
8. Scroll back to the first slice that represents the top of the region of interest.



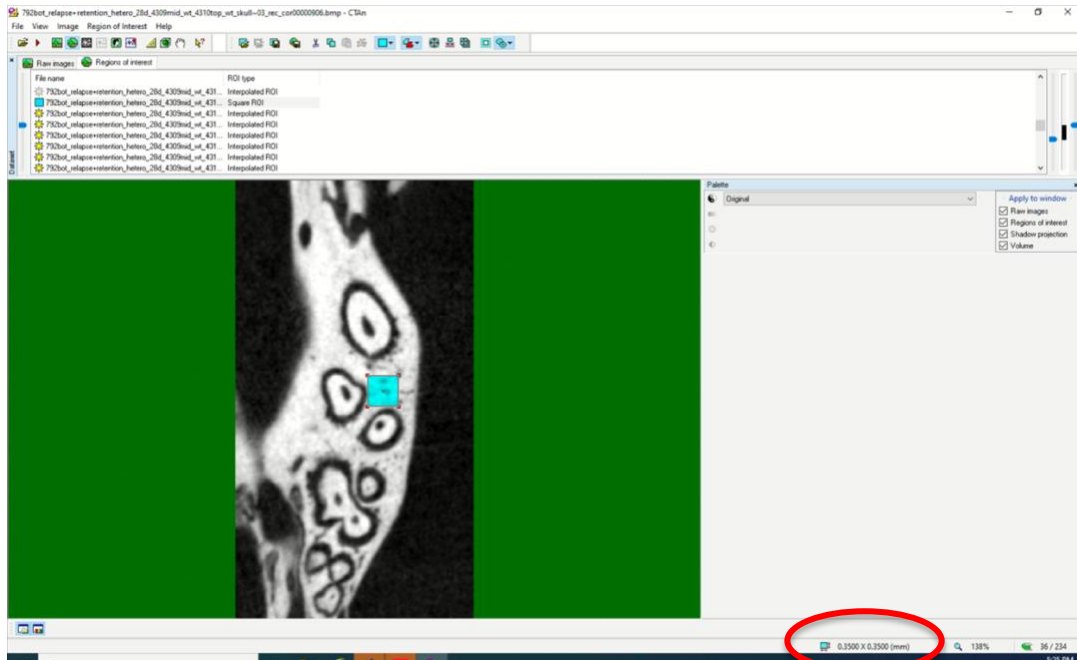
9. Select the square shape to define the area of interest.



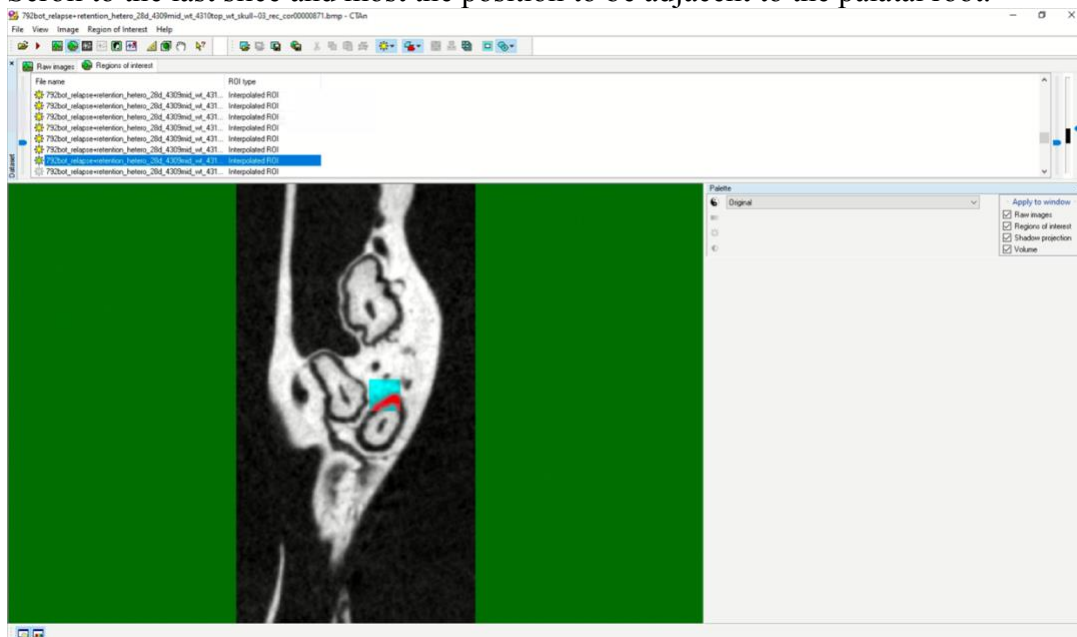
10. Select Dynamic interpolation



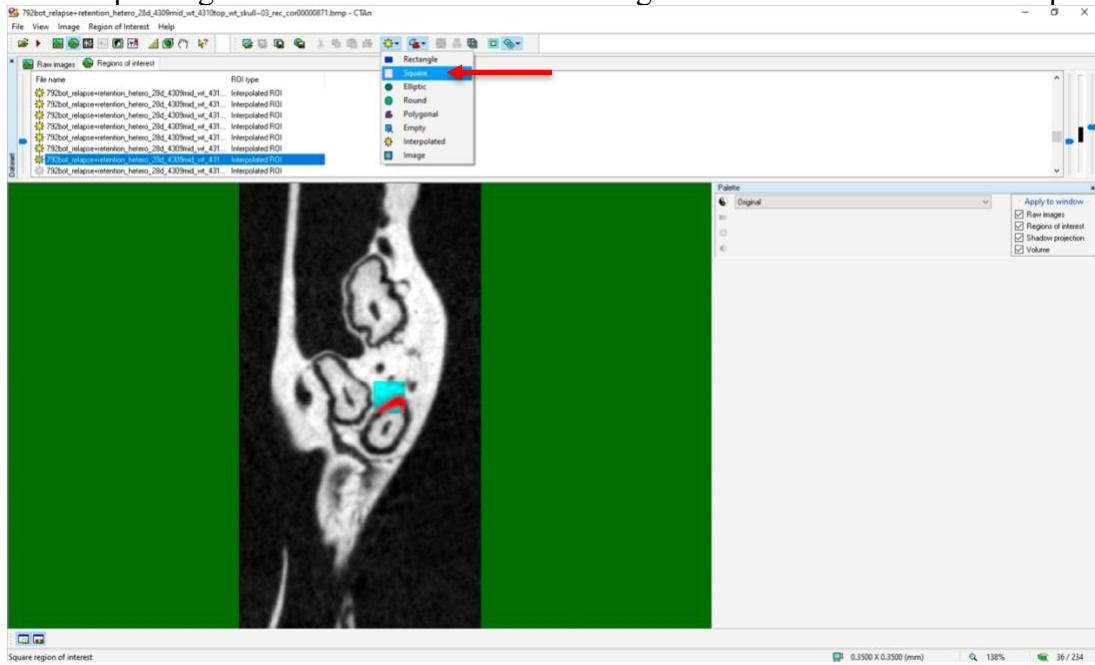
11. Shrink the square region of interest to be **0.35 by 0.35 mm**. Position the square adjacent to the palatal root and be sure to note the square is not in the PDL space of the palatal root or distal root.



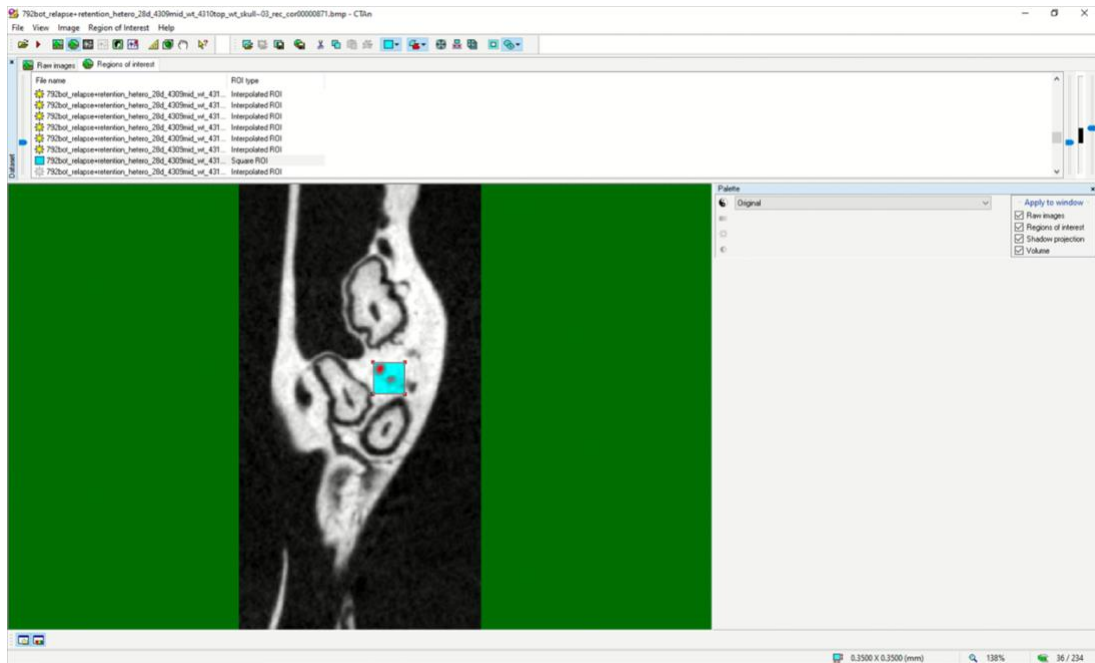
12. Scroll to the last slice and most the position to be adjacent to the palatal root.



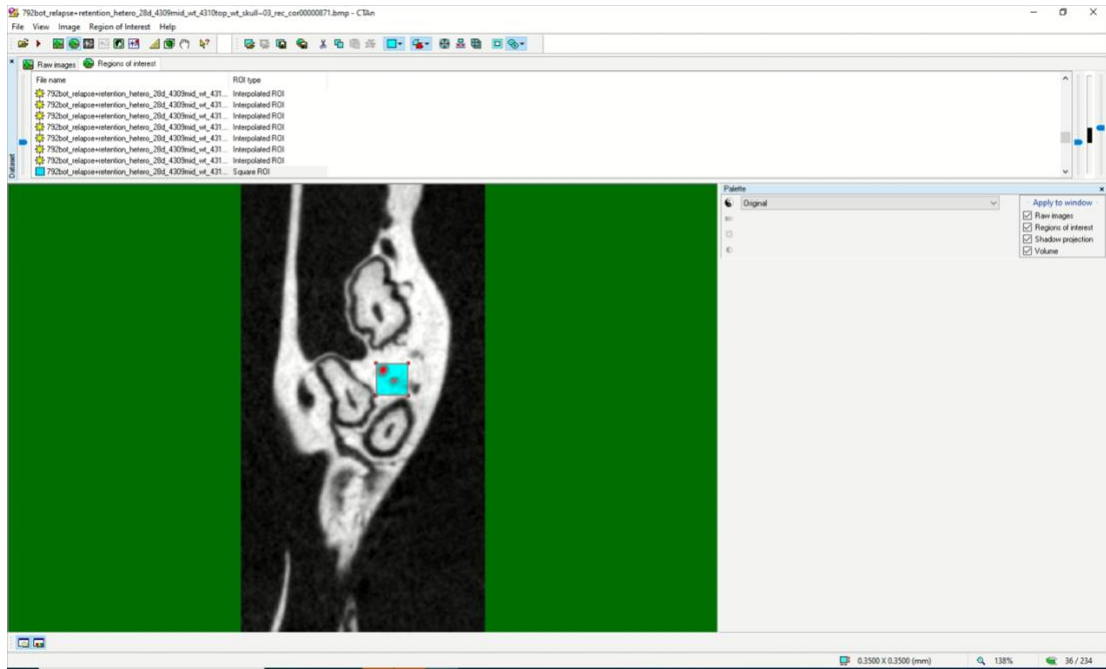
13. Select square again to have access to move the region of interest out of the PDL space.



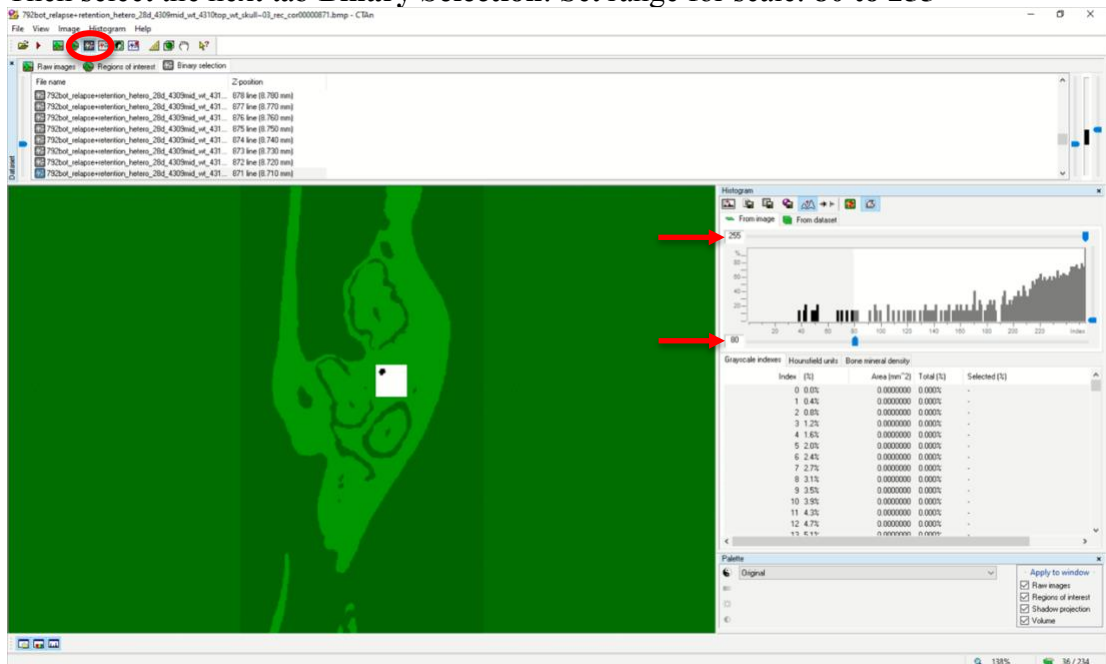
14. Move the region of interest to adjacent to the palatal root and make sure it is not in the PDL.



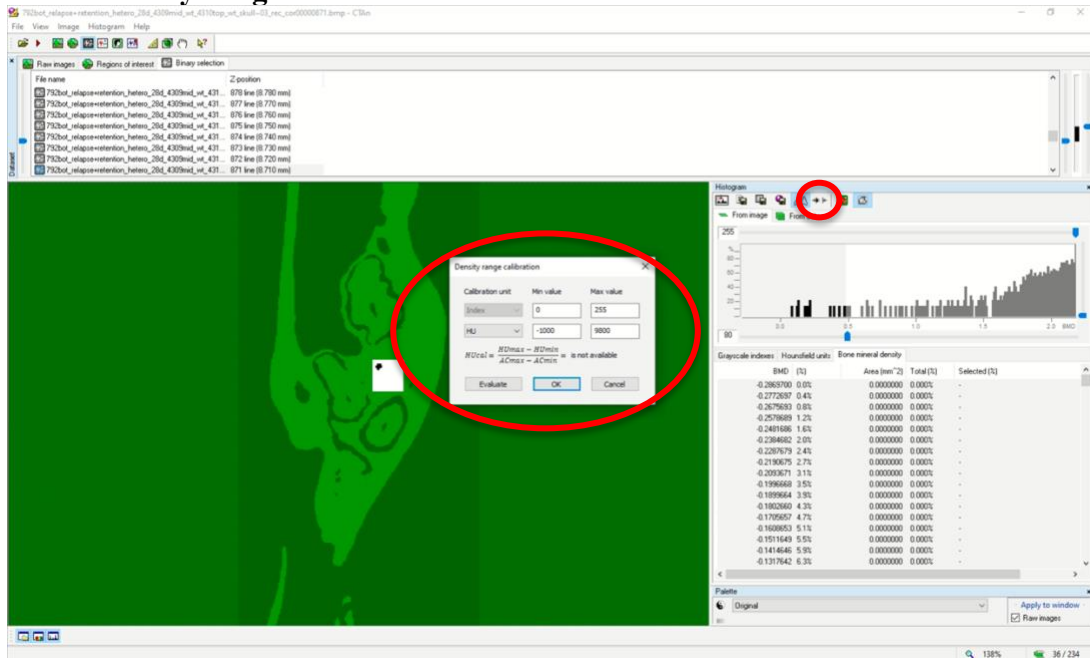
15. Scroll through all the samples to make sure the region of interest is not within the PDL of the root.



16. Then select the next tab **Binary Selection**. Set range for scale: **80 to 255**

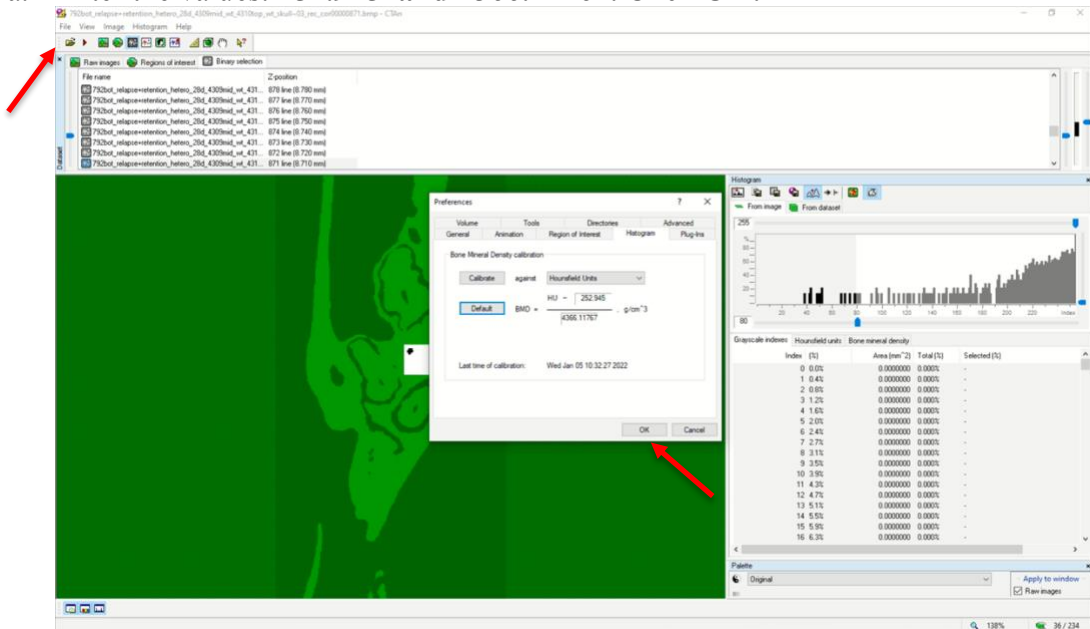


17. Select **Density range calibration**. Set the HU units to **-1000** to **9800**. Click **OK**.

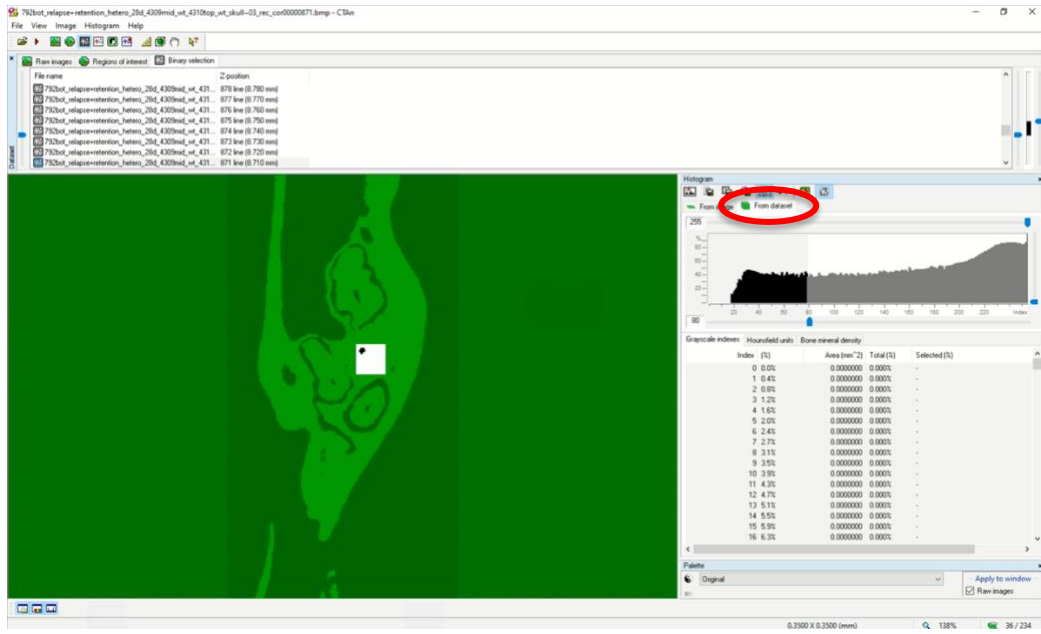


18. Click on File → Preferences → Histogram

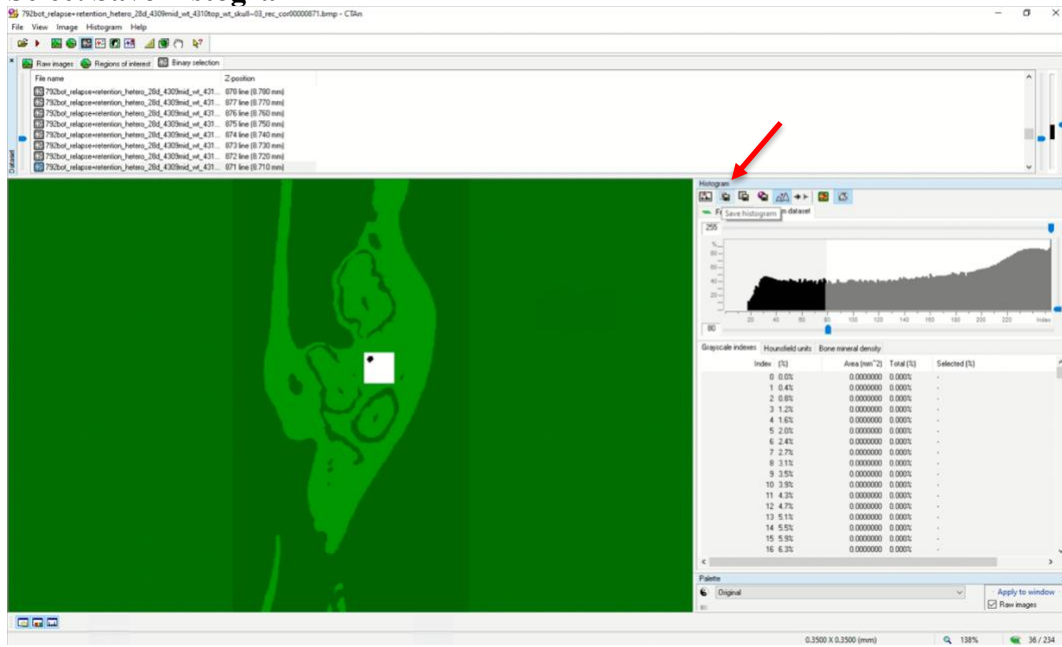
a. Enter the values: **252.945** and **4366.11767**. Click **OK**.



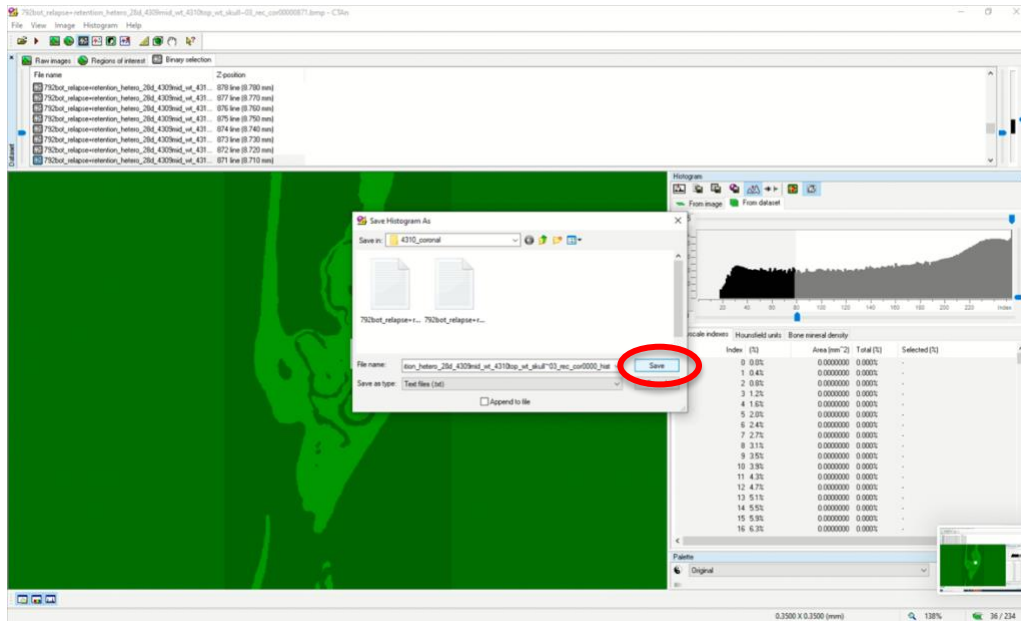
19. Select From Dataset



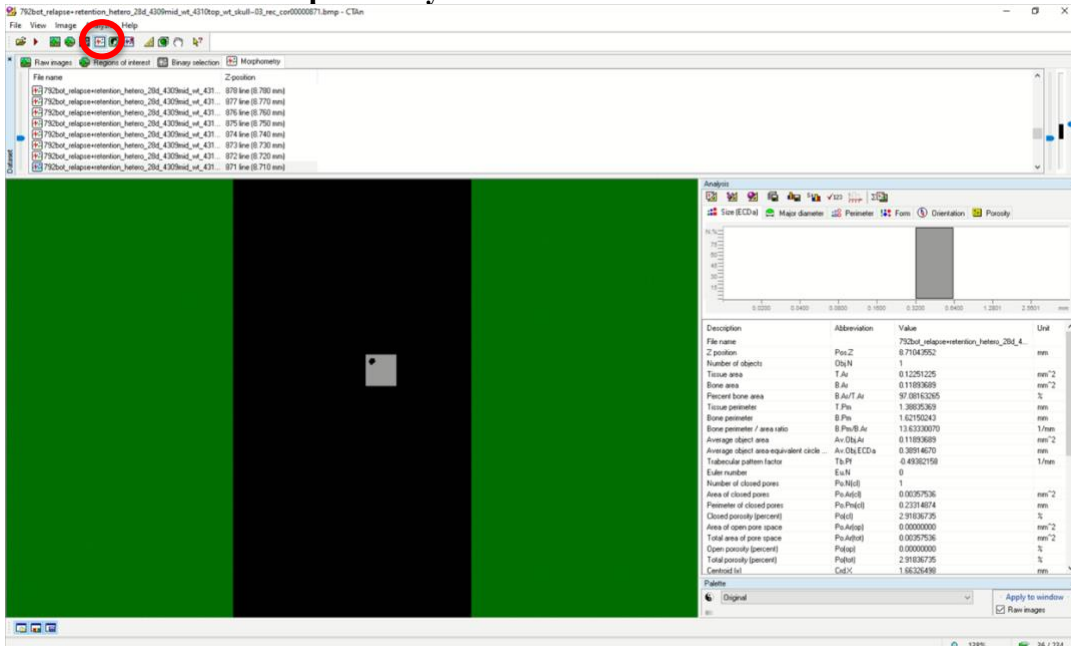
20. Select Save histogram



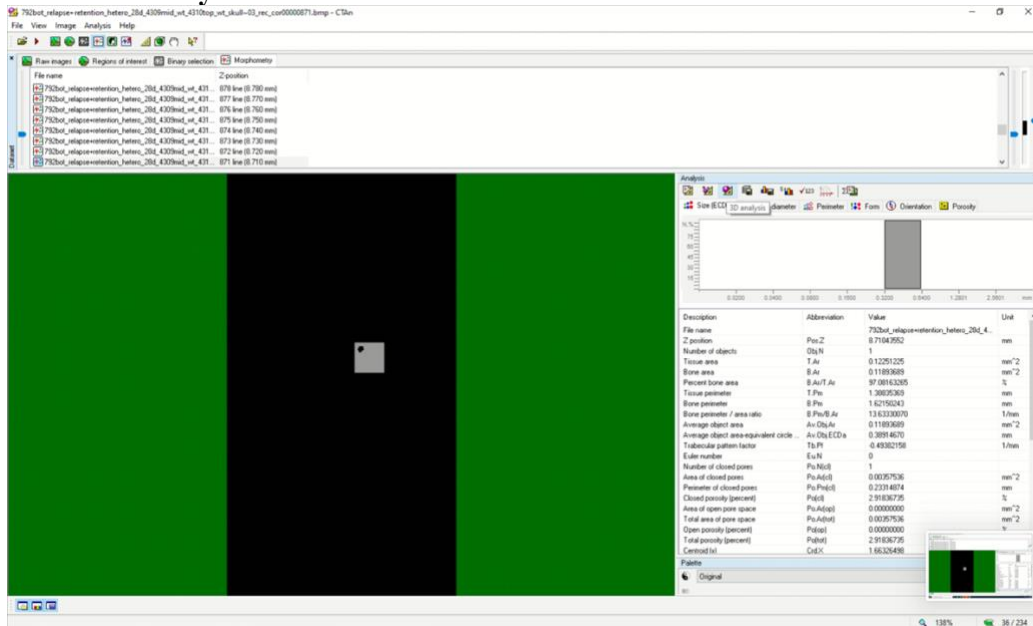
21. Select the folder to save the values from the volumetric data. Click **Save**



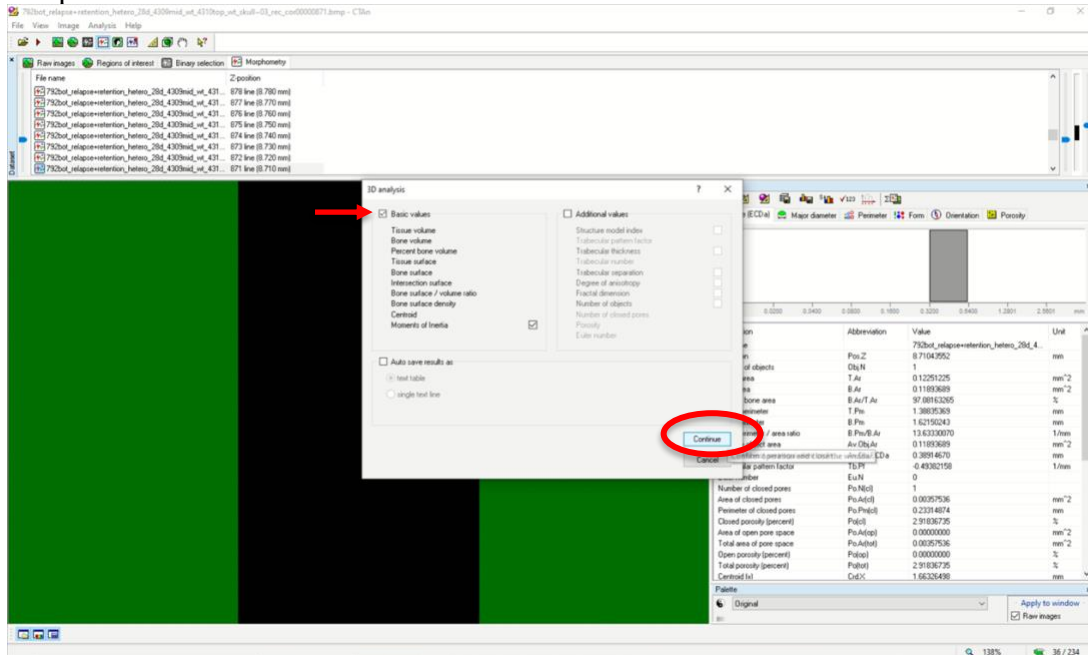
22. Select the next tab **Morphometry**



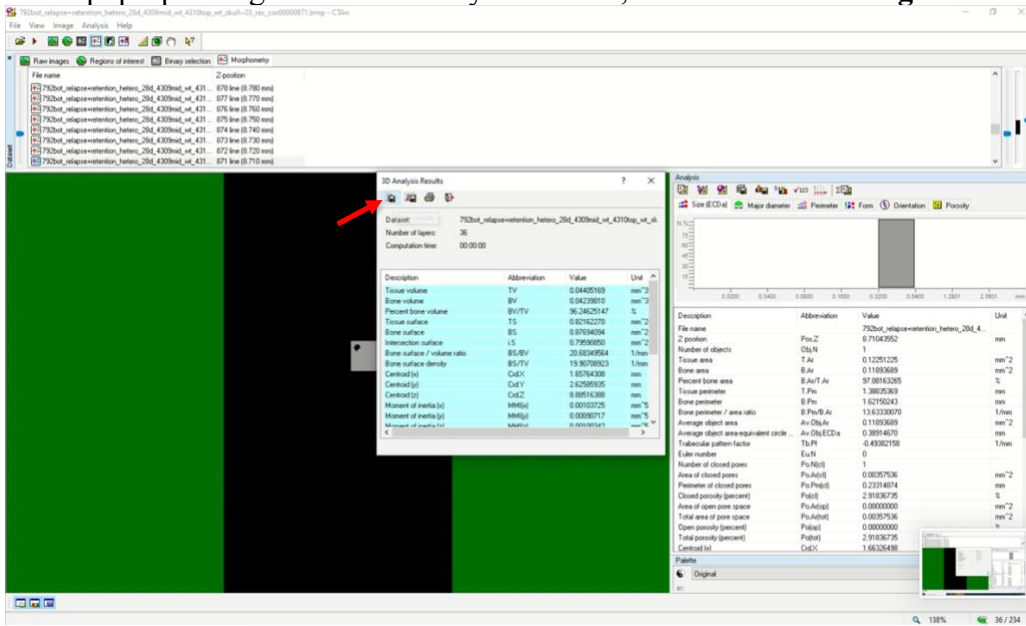
23. Select 3D analysis



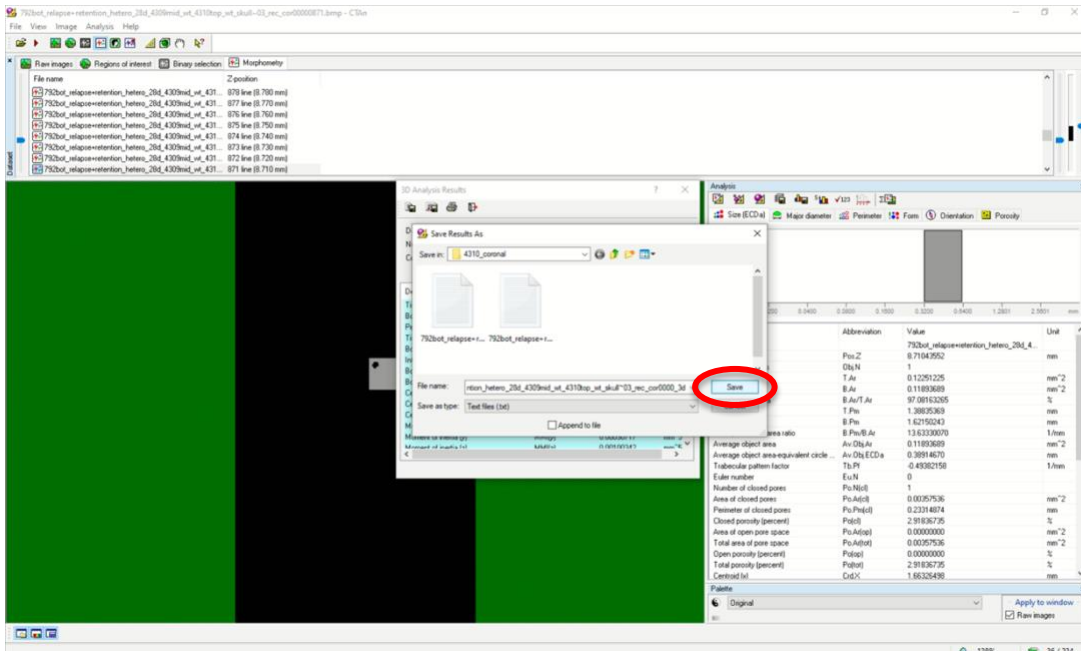
24. Keep the **Basic Values** checked. Click **Continue**



25. In the pop-up dialogue box 3D Analysis Results, select the **save histogram icon**.



26. Select the folder desired and **Save** the results



27. Find the value for **BMD** under the selection, listed as the mean. Enter this value into an excel spreadsheet to keep values organized per sample.

```

3808bot_wt_3999mid_4101top_ko_skull_rec_tra_cor0000_hist - Notepad
File Edit Format View Help
1.8665113,87.15,0.0197000,0.447%,0.499%
1.8762117,87.55,0.0164000,0.338%,0.377%
1.8859120,87.05,0.0161000,0.365%,0.408%
1.8956124,88.25,0.0184000,0.417%,0.466%
1.9053128,88.05,0.0197000,0.447%,0.499%
1.9150131,89.05,0.0191000,0.433%,0.483%
1.9247135,89.45,0.0166000,0.376%,0.420%
1.9344139,89.85,0.0203000,0.460%,0.514%
1.9441142,90.25,0.0216000,0.490%,0.547%
1.9538146,90.65,0.0172000,0.390%,0.435%
1.9635150,91.05,0.0203000,0.460%,0.514%
1.9732153,91.45,0.0199000,0.453%,0.504%
1.9829157,91.85,0.0211000,0.478%,0.534%
1.9926161,92.25,0.0196000,0.444%,0.496%
2.0023164,92.55,0.0206000,0.467%,0.521%
2.0120168,92.95,0.0257000,0.583%,0.651%
2.0217172,93.35,0.0249000,0.565%,0.630%
2.0314175,93.75,0.0255000,0.578%,0.645%
2.0411179,94.15,0.0259000,0.583%,0.651%
2.0508183,94.55,0.0264000,0.599%,0.668%
2.0605186,94.95,0.0286000,0.649%,0.724%
2.0702190,95.35,0.0292000,0.662%,0.739%
2.0799194,95.75,0.0293000,0.664%,0.742%
2.0896197,96.15,0.0293000,0.664%,0.742%
2.0993201,96.55,0.0342000,0.776%,0.866%
2.1090205,96.95,0.0378000,0.87%,0.957%
2.1187208,97.35,0.0431000,0.977%,1.091%
2.1284212,97.75,0.0452000,1.025%,1.144%
2.1381216,98.15,0.0464000,1.052%,1.175%
2.1478219,98.55,0.0570000,1.293%,1.443%
2.1575223,98.95,0.0715000,1.621%,1.818%
2.1672227,99.35,0.0908000,2.059%,2.298%
2.1769230,99.75,0.1557000,3.513%,3.941%
2.1866234,100.05,1.6459000,37.322%,41.662%
***
Mean (total): 1.7068210,,'
Selection,,'
Begin: 0.4890993,,'
End: 1.866214,,'
Number of voxels: 39506,,'
Mean: 1.8916184,,'
Standard deviation: 0.4431048,,'
Standard error of mean: 0.0022258,,'
95% confidence limits,,'
Minimum: 1.8871588,,'
Maximum: 1.8966708,,'

```

28. Find the value for **BV** and **BV/TV** under the selection, listed as the mean. Enter this value into an excel spreadsheet to keep values organized per sample.

```

3808bot_wt_3999mid_4101top_ko_skull_rec_tra_cor0000_3d - Notepad
File Edit Format View Help
IT Analyser, Version: 1.18.8.0
Date and time, 06.03.2022 17:48
Operator identity, jfaldu
Computer name, OFS-418522-SW
Computation time, 00:00:01
Dataset, 3808bot_wt_3999mid_4101top_ko_skull_rec_tra_cor-0000
Location, I:\Baseline Samples Data\3809_coronal\

Description, Abbreviation, Value, Unit
Number of layers, 36
Lower vertical position, 8.1500000, mm
Upper vertical position, 8.5000000, mm
Pixel size, 10.0000000, um
Lower grey threshold, 80
Upper grey threshold, 255

Tissue volume, TV, 0.04404708, mm^3
Bone volume, BV, 0.03947213, mm^3
Percent bone volume, BV/TV, 89.61350070, %
Tissue surface, TS, 0.79609091, mm^2
Bone surface, BS, 0.90018218, mm^2
Intersection surface, IS, 0.67959511, mm^2
Bone surface / volume ratio, BS/BV, 22.80551131, 1/mm
Bone surface density, BS/TV, 20.43681703, 1/mm
Centroid (x), Crd. X, 1.69389232, mm
Centroid (y), Crd. Y, 2.87210095, mm
Centroid (z), Crd. Z, 8.33373943, mm
Moment of inertia (x), MMI(x), 0.00087950, mm^5
Moment of inertia (y), MMI(y), 0.00082232, mm^5
Moment of inertia (z), MMI(z), 0.00087243, mm^5
Polar moment of inertia, MMI(polar), 0.00128712, mm^5
Radius of gyration (x), Gr. R(x), 0.14928626, mm
Radius of gyration (y), Gr. R(y), 0.14427400, mm
Radius of gyration (z), Gr. R(z), 0.14860496, mm
Polar radius of gyration, Gr. R(polar), 0.18058060, mm
Product of inertia (xy), Pr. In(xy), -0.00001209, mm^5
Product of inertia (xz), Pr. In(xz), 0.00003694, mm^5
Product of inertia (yz), Pr. In(yz), -0.00014974, mm^5
Total orientation (theta), T. O(theta), 49.83111305, °
Total orientation (phi), T. O(phi), 283.88320249, °

```

B9: Statistical Analysis

Statistical evaluation was performed with the program GraphPad Prism (V9.3.1). Data was expressed as means and standard deviations for each group and subjected to two-way ANOVA followed by a Tukey test for multiple comparisons among the Dmp1-Cre^{-/-};Tbr2^{fl/fl} and Dmp1-Cre^{+/-};Tbr2^{fl/fl} groups ($p=0.05$). Gender comparisons tested with unpaired T-test ($p= 0.05$) for each parameter.

C: RESULTS

C1: Final Sample Size

Table 1: Breakdown of samples included in the statistical analysis.

n	Female Groups	n	Male Groups
8	Control Dmp1-Cre ^{-/-} ;Tbr2 ^{fl/fl}	7	Control Dmp1-Cre ^{-/-} ;Tbr2 ^{fl/fl}
3	Control Dmp1-Cre ^{+/-} ;Tbr2 ^{fl/fl}	3	Control Dmp1-Cre ^{+/-} ;Tbr2 ^{fl/fl}
3	OTM Dmp1-Cre ^{-/-} ;Tbr2 ^{fl/fl}	8	OTM Dmp1-Cre ^{-/-} ;Tbr2 ^{fl/fl}
5	OTM Dmp1-Cre ^{+/-} ;Tbr2 ^{fl/fl}	3	OTM Dmp1-Cre ^{+/-} ;Tbr2 ^{fl/fl}

C2: MicroCT Analysis Results

All mice in the study remained healthy and had a slight increase or maintained body weight throughout the 14-day experimental period. Prior to comparing samples with OTM, non-experimental samples were analyzed. Our non-experimental groups will be referred to as baseline samples for the male and female Dmp1-Cre^{-/-};Tbr2^{fl/fl} groups and male and female Dmp1-Cre^{+/-};Tbr2^{fl/fl} groups. These graphs in Figure 3 represent baseline samples that did not undergo any OTM or anesthesia. The lighter color bar represents the Dmp1-Cre^{-/-};Tbr2^{fl/fl} group and the darker color bar represents the Dmp1-Cre^{+/-};Tbr2^{fl/fl} group. There is no statistically significant difference in bone quality between genotypes within the same gender as seen in Figure 3.

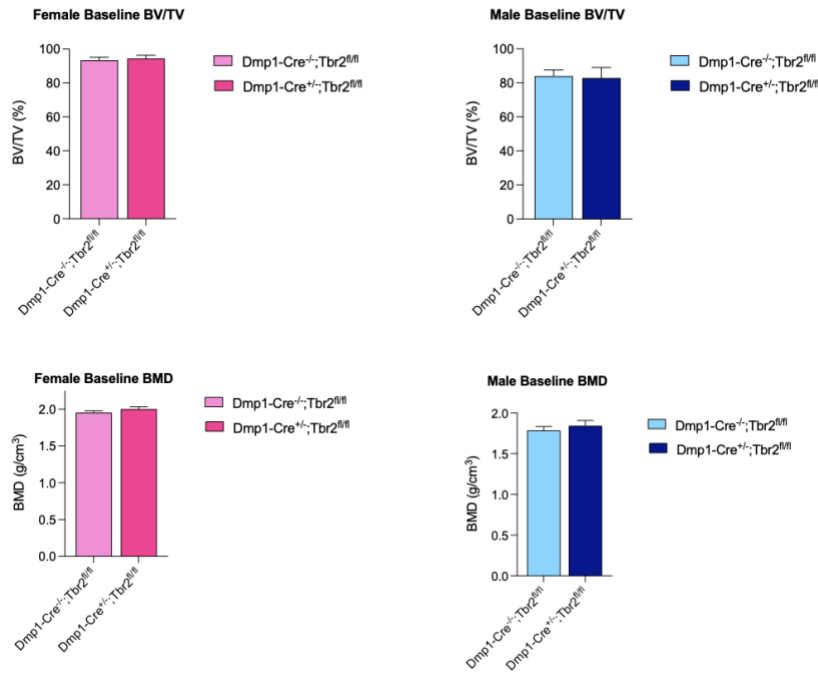


Figure 3: Graphical representation of the baseline groups split by male and female for Dmp1-Cre^{-/-};Tbr2^{fl/fl} and Dmp1-Cre^{+/-};Tbr2^{fl/fl} groups. No statistically significant findings were noted.

Comparisons of the baseline mice were done within the same genotype between genders. The females in Dmp1-Cre^{-/-};Tbr2^{fl/fl} group showed higher bone volume fraction ($*p \leq 0.05$) and bone mineral density ($**p \leq 0.01$) in the bone of the furcation area as seen in Figure 4. The females in Dmp1-Cre^{+/-};Tbr2^{fl/fl} group showed higher bone volume fraction ($*p \leq 0.05$) and bone mineral density ($*p \leq 0.05$) in the bone of the furcation area as seen in Figure 5.

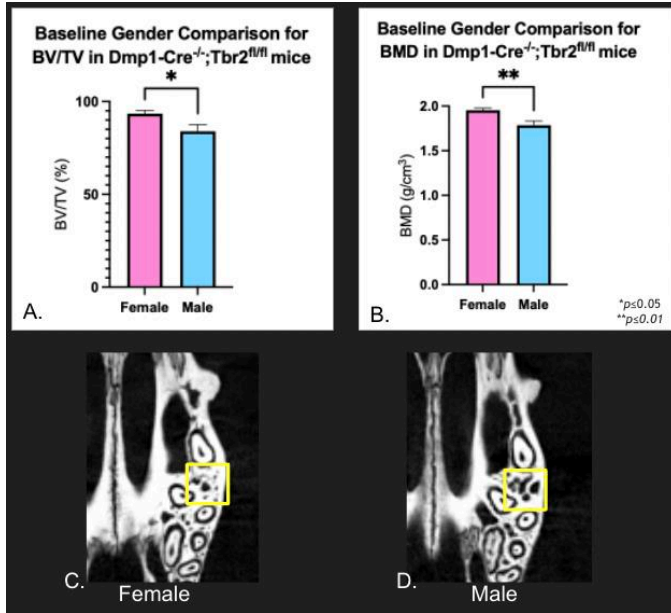


Figure 4: A. Baseline gender comparison for BV/TV in Dmp1-Cre^{-/-};Tbr2^{fl/fl} mice. B. Baseline gender comparison for BMD in Dmp1-Cre^{-/-};Tbr2^{fl/fl} mice. C. Coronal cross-section of maxillary left side first molar at the level of the furcation area in female Dmp1-Cre^{-/-};Tbr2^{fl/fl} mice. D. Coronal cross-section of maxillary left side first molar at the level of the furcation area in male Dmp1-Cre^{-/-};Tbr2^{fl/fl} mice.

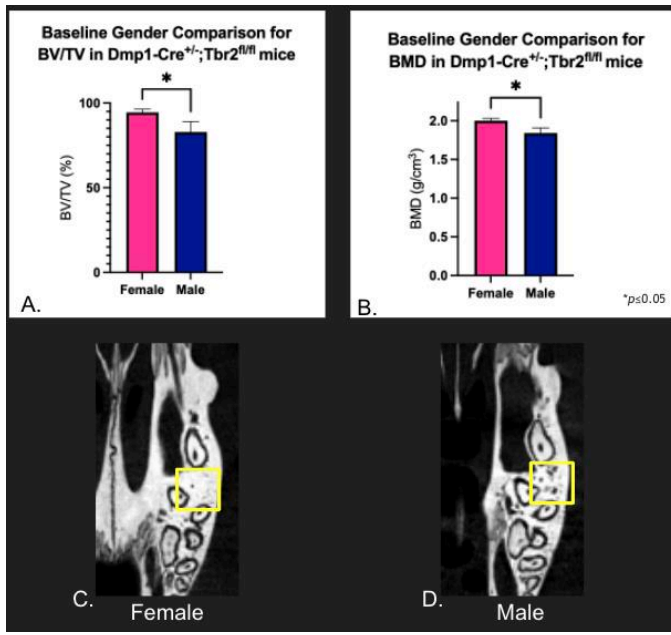


Figure 5: A. Baseline gender comparison for BV/TV in Dmp1-Cre^{+/-};Tbr2^{fl/fl} mice. B. Baseline gender comparison for BMD in Dmp1-Cre^{+/-};Tbr2^{fl/fl} mice. C. Coronal cross-section of maxillary left side first molar at the level of the furcation area in female Dmp1-Cre^{+/-};Tbr2^{fl/fl} mice. D. Coronal cross-section of maxillary left side first molar at the level of the furcation area in male Dmp1-Cre^{+/-};Tbr2^{fl/fl} mice.

The OTM rate was also compared between the two genotypes with respect to the gender. 3 samples needed to be excluded due to distal molar breakage during spring removal for microCT scan and were not included in Table 1. The control represents the group of mice that did not receive the orthodontic appliance, therefore the distance between the first and second molar is plotted as zero (Figure 6). Our results for OTM distance for Dmp1-Cre^{-/-};Tbr2^{fl/fl} groups

for females ($120.68 \pm 14.12 \mu\text{m}$) and for males ($138.11 \pm 26.41 \mu\text{m}$) illustrated a much smaller range of tooth movement compared to $\text{Dmp1-Cre}^{+/-};\text{Tbr2}^{\text{fl/fl}}$ groups for females ($141.07 \pm 61.31 \mu\text{m}$) and males ($186.81 \pm 112.22 \mu\text{m}$). Although there is no statistical difference in OTM rate between the two genotypes, you can see the large variation in OTM in the male $\text{Dmp1-Cre}^{+/-};\text{Tbr2}^{\text{fl/fl}}$ group, which can be due to the defective TGF β signaling that makes bone remodeling unpredictable, since the process is dysregulated.

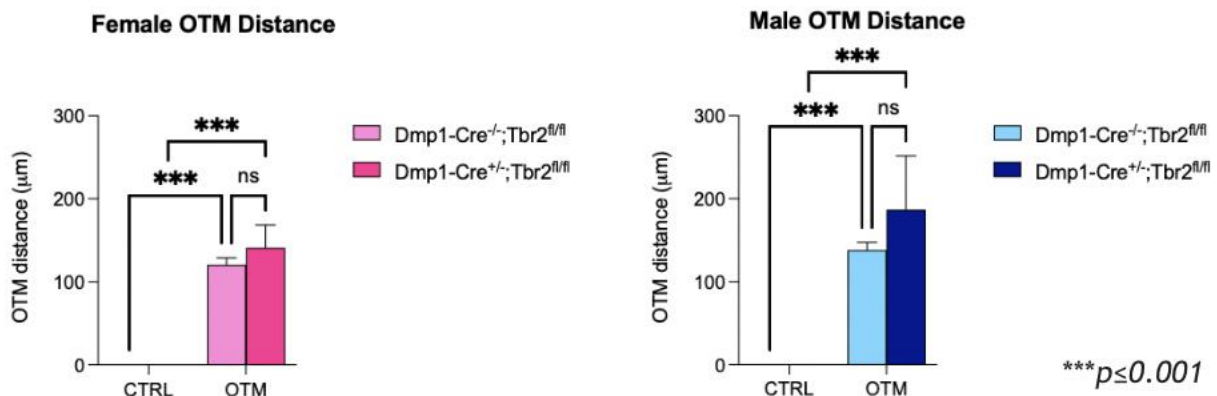


Figure 6: Graphical representation of orthodontic tooth movement linear measurements between genotypes when split by gender.

When comparing bone quality within the same gender for two different genotypes there was no difference calculated in bone volume fraction or BMD in females. The findings showed that the $\text{Dmp1-Cre}^{+/-};\text{Tbr2}^{\text{fl/fl}}$ group had slightly greater bone volume fraction and bone mineral density compared to the $\text{Dmp1-Cre}^{-/-};\text{Tbr2}^{\text{fl/fl}}$ group for both control and OTM groups as seen in Figure 7. In males, there was a decreased bone volume fraction and BMD in the OTM groups compared to the controls for both genotypes. The OTM $\text{Dmp1-Cre}^{+/-};\text{Tbr2}^{\text{fl/fl}}$ group showed the least amount of BV/TV and BMD highlighted in Figure 8.

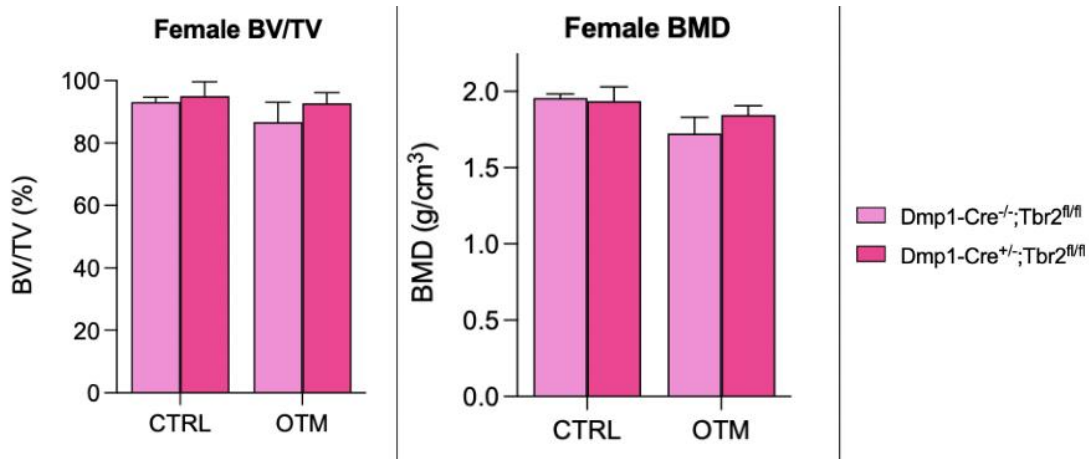


Figure 7: Female control and OTM groups comparison between genotypes for bone quality.

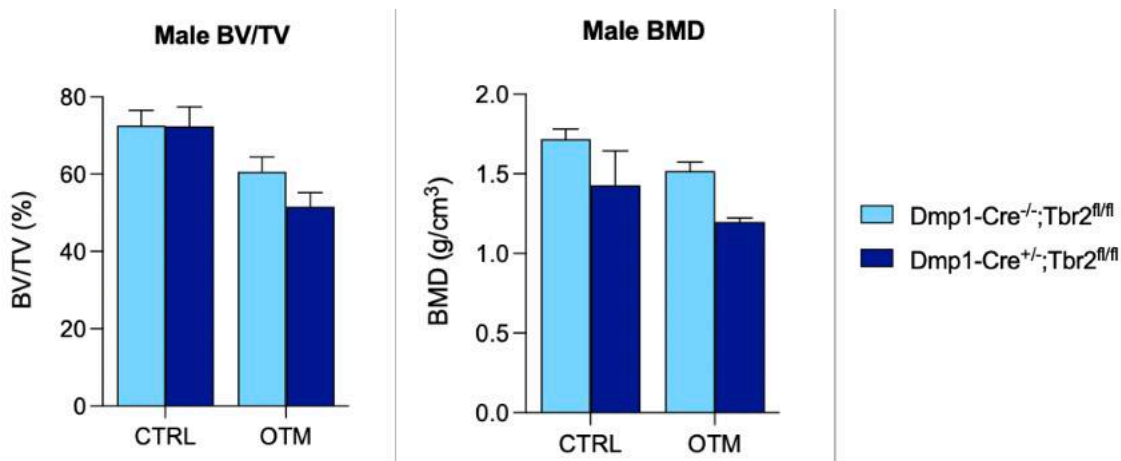


Figure 8: Male control and OTM groups comparison between genotypes for bone quality.

The gender comparison within the same genotype of mice that experienced OTM yielded a statistically significant difference in the bone quality for bone volume fraction in both Dmp1-Cre^{-/-};Tbr2^{fl/fl} (** $p \leq 0.01$) and Dmp1-Cre^{+/-};Tbr2^{fl/fl} groups (** $p \leq 0.001$). The female mice have higher bone volume fraction and BMD compared to males in both genotypes following 14 days of OTM (Figure 9).

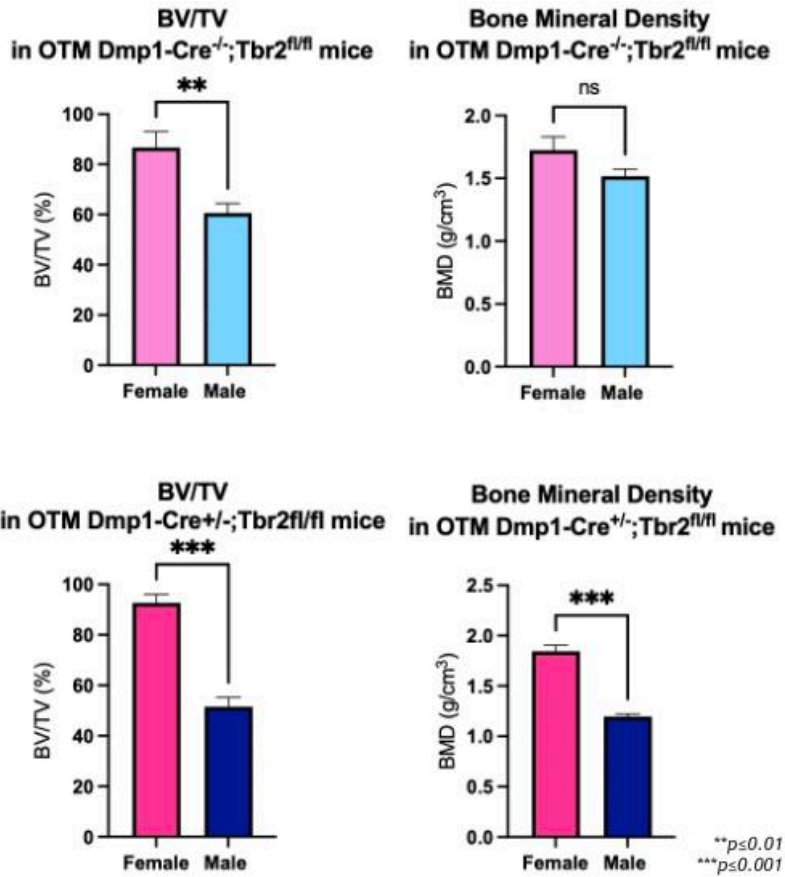


Figure 9: Graphical comparison of BV/TV and BMD between genders within the same genotype after 14 days of orthodontic tooth movement.

Overall, the summary of the findings shed light on the differences between gender alveolar bone quality after TGFβ signaling is impaired in osteocytes. At baseline there was no statistically significant difference in bone quality between genotypes within the same gender. However, at baseline there was a statistically significant difference in alveolar bone quality between females and males. OTM measurements had larger variation in Dmp1-Cre^{+/-};Tbr2^{fl/fl} groups compared to Dmp1-Cre^{-/-};Tbr2^{fl/fl} group potentially due to the dysregulation of TGFβ signaling. In males, there was a decreased BV/TV and BMD in alveolar bone in the OTM group compared to control for both genotypes.

D: DISCUSSION

Orthodontists rely on a homeostasis between bone resorption and bone formation to make changes to tooth position. However, once orthodontic treatment is completed, being able to maintain final tooth position is still challenging. The importance of understanding the mechanisms of OTM and alveolar bone remodeling to increase efficiency of tooth movement and decrease treatment time is another challenging issue in orthodontics. Gaining a further understanding of the molecular mechanisms at play during alveolar bone remodeling is a step towards innovative therapies to address these obstacles. TGF β mediates the crosstalk between osteoclasts and osteoblasts during bone remodeling and supports a healthy bone matrix, and osteocytes help in the regulation of these processes [6] [8] [11] [13]. There are many studies that support the important role TGF β has during osteogenesis focusing on cortical and trabecular bone [44] [45] [36] [46]. Xu et. al. highlights T β RII is critical for osteogenic progenitor cell proliferation and differentiation during postnatal alveolar bone formation [47]. This study provides insight and support as to how bone quality was impacted with loss of TGF β signaling. Therefore, this study used a genetic model of osteocyte-specific deletion of T β RII to show how the loss of osteocyte-intrinsic TGF β signaling affects the alveolar bone during OTM.

In order to establish an OTM model to study, we utilized the mouse OTM models highly regarded in the literature [7] [9] [38] [39] [48]. Kirschneck et. al. concluded that to induce reliable OTM in mice beyond 7 days, a NiTi coil spring is the method of choice. They shared, in comparison to an elastic module for tooth separation, the insertion of a NiTi coil spring was more time-consuming and technically demanding, but best for long-term experiments. Since this study was a 14-day period to establish tooth movement of the first maxillary molar, it was critical to use a reliable method that induced tooth movement continuously. Despite the setbacks

of the NiTi coil spring appliance explained by Kirschneck there are many benefits of this approach compared to the elastic module. Once the elastic module is no longer compressed and the teeth move, it falls out of the mouth and does not retain the OTM achieved [48]. We were able to maintain a NiTi coil spring appliance in the mice for 14 day period for the samples analyzed in this paper with the similar approach used by many [7] [8] [9] [38]. The NiTi coil spring appliance was held securely in place with stainless steel ligature ties on both the first molar and central incisors to ensure mechanical retention. We also added 0.5mm grooves with a high-speed handpiece on the distal side of both central incisors for the ligature tie to stay securely in place. To help ensure the appliance could withstand mastication, we added bonding agent and composite to each tooth to serve as secondary retention. This model allowed us to successfully induce OTM in the mice for a 14-day period.

Our baseline OTM linear measurements data was comparable to those found in the literature [38]. The maxillary first molar moved mesially with a small range in our female ($\pm 14.12 \mu\text{m}$) and male ($\pm 26.41 \mu\text{m}$) $\text{Dmp1-Cre}^{-/-};\text{Tbr2}^{\text{fl/fl}}$ mice (Figure 6). This data helps support the OTM model used in this study and illustrates how OTM can be reproduced in a reliable way. Interestingly, our range for OTM distance in $\text{Dmp1-Cre}^{+/-};\text{Tbr2}^{\text{fl/fl}}$ group ($\pm 112.2 \mu\text{m}$) can potentially be supported by the unpredictable reaction of alveolar bone remodeling (Figure 6). Since osteocytes are not functioning properly with lack of TGF β signaling, there is no homeostasis reached within the bone remodeling process. This can lead to a larger range of reaction to the orthodontic force induced through the NiTi coil spring application. Variability of results can be expected since the downstream influence of TGF β signaling on bone remodeling is disrupted especially during this non-homeostatic condition [11] [49].

At baseline comparison between the genotypes showed no significant difference in BV/TV or BMD (Figure 3). Baseline comparison of male to female bone quality in $Dmp1-Cre^{+/-};Tbr2^{fl/fl}$ mice illustrated females have a higher bone volume fraction and bone mineral density. Dole et. al. shared sexual dimorphism is present in $TGF\beta$'s regulation of osteocyte PLR activity, which helps support these findings. The loss of osteocyte-intrinsic $TGF\beta$ signaling affects the skeleton of male, but not female, mice in homeostatic conditions of long bones [49]. These findings indicate that female mouse bones do not depend on osteocytic $TGF\beta$ signaling for maintaining bone mass and quality. Our observations support that osteocyte-intrinsic $TGF\beta$ impacts alveolar bone in a sexually dimorphic manner. Our findings of sexual dimorphism are present in both homeostatic condition and during OTM, which is inducing minor injury to the PDL area and bone to induce bony change (Figure 9). This created an environment that is not balanced and relies on the bone remodeling process to regulate. Our OTM groups of $Dmp1-Cre^{+/-};Tbr2^{fl/fl}$ genotype illustrates bone volume fraction and bone mineral density is statistically ($***p<0.05$) higher in females than males (Figure 9). Due to intrinsic gender differences in bone quality and response to osteocyte-intrinsic $TGF\beta$ signaling disruption, the sample groups needed to be separated into male and female groups as we did in this study. Although this decreased the overall sample size used for statistical evaluation, these findings are more accurate than combining the genders with different bone qualities into one group. Combining sample groups with different genders can potentially drastically skew results.

The gender differences we noted in alveolar bone are the opposite of findings in the literature for long bones [50] [51] [52]. Differences in BV/TV and BMD were statistically significant ($***p<0.05$) between male and female, with females exhibiting greater bone qualities. Yao et. al. noted when studying the tibia, which is a long bone, that male mice had inherently

more bone volume than genotype-matched female counterparts with corresponding increases in bone biomechanical strength [50]. They shared that the structure and geometry in bone growth, pubertal growth changes, and bone mechanical properties differed in males and females leading to these findings. Ko et. al. also found skeletal unloading diminishes bone quality in the tibia and fibula, leading to an increase in bone fracture risks, particularly in females [51]. The gender differences we see in this study for the alveolar bone are the opposite in long bone.

Alveolar bone and long bone respond differently to loading and unloading forces. Other bones in the body resorb or narrow under tension and widen or build under compression. This is in accordance with the long bone viscoelastic and anisotropic properties [53]. Depending on the direction the force is applied to the long bones there is a specific response. Alveolar bone responds with the opposite reaction. Under tension alveolar bone apposition occurs with the help of osteoblasts and under compression the area attracts osteoclasts which resorb the bone [1] [14] [19] [21] [17] [2] [16].

It is interesting to point out that when alveolar bone and long bones are compared within the same mouse, like the study by Chen et. al. it was found that there was no evidence of extensive bone loss in alveolar bone compared to the appendicular skeleton found when comparing aging rats and young, ovariectomized rats. There was clear evidence of osteopenia/osteoporosis in the long bones, but transverse microCT sections through the maxillary alveolar bone did not show the same diminishes in bone properties [54]. This opens the avenue for future studies of these mice to compare areas of cortical bone and trabecular bone to alveolar bone in the $Dmp1-Cre^{+/-};Tbr2^{fl/fl}$ mice.

E: FUTURE DIRECTIONS

There are many future directions this study can launch into. Analyzing these samples for histological changes and molecular mechanisms will allow us to deeper understand the changes that are taking place once osteocyte-intrinsic TGF β signaling is disrupted. Increasing the sample size of the male and female Dmp1-Cre^{+/-};Tbr2^{fl/fl} mice will help increase the power of clinical relevance. Also, considering the use of *in vivo* MicroCT to scan at different stages of tooth movement such as Day 3 and Day 7 without sacrificing samples to learn more about the bone remodeling phases. Further explore gender differences specific to alveolar bone compared to long bones, which can help guide therapeutic decisions in the future. Develop targeted therapy at the level of molecular mechanisms that can influence relapse and retention with our knowledge of OTM mouse model established here.

F: LIMITATIONS

There was difficulty in breeding an abundant number of Dmp1-Cre^{+/-};Tbr2^{fl/fl} mice for orthodontic appliance placement. An increased sample size would help draw stronger conclusions for clinical relevance. Three samples needed to be excluded due to first molar breakage during spring removal for microCT analysis. The high level of technical skill needed to properly place the orthodontic appliance requires training and practice to create consistency. There were also challenges in forward momentum due to the COVID-19 pandemic and consequent clinic and lab closures.

G: CONCLUSIONS

1. Preliminary data is promising and increasing the sample size will help support further scientific discovery and clinical applications.
2. Orthodontic tooth model used in this study with a NiTi coil spring is reliable and reproducible for long term studies.
3. Larger range of orthodontic tooth movement in the $Dmp1-Cre^{+/-};Tbr2^{fl/fl}$ groups compared to $Dmp1-Cre^{-/-};Tbr2^{fl/fl}$ group can be due to the dysregulation of TGF β signaling downstream resulting in variable bone remodeling.
4. Significant differences in alveolar bone quality between males and females compared to long bones properties highlighted in the literature illustrates the importance of separating experimental groups by genotype and phenotype.

H: REFERENCES

- [1] Y. Li, L. A. Jacox, S. H. Little and C.-C. Ko, "Orthodontic tooth movement: the biology and clinical implications," *The Kaohsiung Journal of Medical Sciences*, vol. 34, no. 4, pp. 207-214, 2018.
- [2] M. Meikle, "The tissue, cellular, and molecular regulation of orthodontic tooth movement: 100 years after Carl Sandstedt," *Eur J Orthod*, vol. 28, pp. 221-40, 2006.
- [3] J. King, D. Keeling and T. Wronski, "Histomorphometric study of alveolar bone turnover in orthodontic tooth movement.," *Bone*, vol. 12, pp. 401-9, 1991.
- [4] P. Rygh, "Ultra structural changes in tension zones of rat molar periodontium incident to orthodontic tooth movement," *Am J Orthod*, vol. 70, pp. 269-81, 1976.
- [5] M. Knothe, J. Adamson, A. Tami and T. Bauer, "The osteocyte," *The International Journal of Biochemistry & Cell Biology*, vol. 36, no. 1, pp. 1-8, 2004.
- [6] L. Bonewald, "The amazing osteocyte," *J Bone Miner Res*, vol. 26, no. 2, pp. 229-38, 2011.
- [7] T. Matsumoto, T. Limura, K. Ogura, K. Moriyama and A. Yamaguchi, "The role of osteocytes in bone resorption during orthodontic tooth movement," *J Dent Res*, vol. 92, no. 4, pp. 340-345, 2013.
- [8] S. Moin, Z. Kalajzic and A. Utreja, "Osteocyte death during orthodontic tooth movement in mice," *Angle Orthod*, vol. 84, no. 6, pp. 1086-1092, 2014.
- [9] A. Shoji-Matsunaga, T. Ono, M. Hayashi and H. Takayanagi, "Osteocyte regulation of orthodontic force-mediated tooth movement via RANKL expression," *Sci Rep*, vol. 7, no. 1, p. 8753, 2017.

- [10] M. Prideaux, D. Findlay and G. Atkins, "Osteocytes: The master cells in bone remodelling," *Curr Opin Pharmacol*, vol. 28, pp. 24-30, 2016.
- [11] N. Dole, C. Mazur and C. Acevedo, "Osteocyte-Intrinsic TGF-beta Signaling Regulates Bone Quality through Perilacunar/Canalicular Remodeling," *Cell Rep*, vol. 21, no. 9, pp. 2585-2596, 2017.
- [12] K. Bailey, J. Nguyen, C. Yee, N. Dole, A. Dang and T. Alliston, "Mechanosensitive Control of Articular Cartilage and Subchondral Bone Homeostasis Requires Osteocytic TGFbeta Signaling," *Arthritis Rheumatol*, 2020.
- [13] T. Nakashima, M. Hayashi and T. Fukunaga, "Evidence for osteocyte regulation of bone homeostasis through RANKL expression," *Nature Medicine*, vol. 17, no. 10, pp. 1231-1234, 2011.
- [14] M. Asiry, "Biological aspects of orthodontic tooth movement: A review of literature," *Saudi Journal of Biological Sciences*, vol. 25, pp. 1027-1032, 2018.
- [15] A. Nanci and D. Bosshardt, "Structure of periodontal tissues in health and disease," *Periodontol 2000*, vol. 40, pp. 11-28, 2006.
- [16] S. Baloul, "Osteoclastogenesis and Osteogenesis during Tooth Movement," *Frontiers of oral biology*, vol. 18, pp. 75-79, 2016.
- [17] R. Masella and M. Meister, "Current concepts in the biology of orthodontic tooth movement," *Am J Orthod Dentofacial Orthop*, vol. 129, no. 4, pp. 458-468, 2006.
- [18] S. Henneman, J. Von den Hoff and J. Maltha, "Mechanobiology of tooth movement," *Eur J Orthod*, vol. 30, no. 3, pp. 299-306, 2008.

- [19] C. Burstone, "The biomechanics of tooth movement," *Vistas in orthodontics*, pp. 197-213, 1962.
- [20] O. Tuncay, "Biologic elements of tooth movement," *Quintessence*, 2006.
- [21] V. Krishnan and Z. Davidovitch, "Cellular, molecular, and tissue-level reactions to orthodontic force," *Am. J. Orthod. Dentofacial. Ortho.*, vol. 129, p. 469e.1–460e., 2006.
- [22] S. Al-Ansari, C. Sangsuwon, T. Vongthongleur, R. Kwal, M. Teo, Y. Lee, J. Nervina, C. Teixeira and M. Alikhani, "Biological principles behind accelerated tooth movement," *Seminars Orthod.*, vol. 21, no. 3, pp. 151-161, 2015.
- [23] S. Taddei, I. Andrade and C. Queiroz-Junior, "Role of CCR2 in orthodontic tooth movement," *Am. J. Orthod. Dent. Facial. Orthop.*, vol. 141, no. 2, pp. 153-160, 2012.
- [24] J. Farrar, *Irregularities of the Teeth and Their Correction*, New York: De Vinne Press, 1888.
- [25] C. Bassett and R. Becker, "Generation of electric potentials by bone in response to mechanical stress," *Science*, vol. 137, pp. 1063-1064, 1962.
- [26] A. Zengo, R. Pawluk and C. Bassett, "Stress induced bioelectric potentials in the dentoalveolar complex," *Am. J. Orthod.*, vol. 64, no. 1, pp. 17-27, 1973.
- [27] T. Wada, T. Nakashima, N. Hiroshi and J. Penninger, "RANKL-RANK signaling in osteoclastogenesis and bone disease," *Trends Mol Med*, vol. 12, no. 1, pp. 17-25, 2006.
- [28] S. Dallas, M. Prideaux and L. Bonewald, "The Osteocyte: An Endocrine Cell ... and More," *Endocrine Reviews*, vol. 34, no. 5, p. 658–690, 2013.
- [29] C. Jacobs, S. Temiyasathit and A. Castillo, "Osteocyte mechanobiology and pericellular mechanics," *Annu Rev Biomed Eng*, vol. 12, pp. 369-400, 2010.

- [30] G. Goulet, D. Cooper, D. Coombe and R. Zernicke, "Influence of cortical canal architecture on lacunocanalicular pore pressure and fluid flow," *Comput Meth Biomech Biomed Eng*, vol. 11, pp. 379-87, 2008.
- [31] Y. Nishiyama, T. Matsumoto, J. Lee, T. Saitou, T. Imamura and K. Moriyama, "Changes in the spatial distribution of sclerostin in the osteocytic lacuno-canalicular system in alveolar bone due to orthodontic forces[...]," *Arch Oral Biol*, vol. 60, pp. 45-54, 2015.
- [32] O. Verborgt, G. Gibson and M. Schaffler, "Loss of osteocyte integrity in association with microdamage and bone remodeling after fatigue in vivo," *J Bone Miner Res.*, vol. 15, no. 1, pp. 60-7, 2000.
- [33] G. Kogianni, V. Mann and B. Noble, "Apoptotic bodies convey activity capable of initiating osteoclastogenesis and localized bone destruction," *J Bone Miner Res*, vol. 23, pp. 915-927, 2008.
- [34] S. Dallas, T. Alliston and L. Bonewald, "Transforming growth factor-beta," in *Bone Biology*, San Diego, Academic Press, 2008, p. 1145–1166.
- [35] A. Borton, J. Frederick, M. Datto, X. Wang and R. Weinstein, "The loss of Smad3 results in a lower rate of bone formation and osteopenia through dysregulation of osteoblast differentiation and apoptosis," *J Bone Miner Res*, vol. 16, p. 1754–1764, 2001.
- [36] Y. Tang, X. Wu, W. Lei, L. Pang, C. Wan and Z. Shi, "TGF-beta1-induced migration of bone mesenchymal stem cells couples bone resorption with formation," *Nat Med*, vol. 15, pp. 757-765, 2009.

- [37] A. Simpson, M. Stoddart, C. Davies, K. Jahn, P. Furlong and J. Gasser, "TGF β 3 and loading increases osteocyte survival in human cancellous bone cultured ex vivo," *Cell Biochem Funct*, vol. 27, pp. 23-29, 2009.
- [38] S. Yadav, T. Dobie, A. Assefnia, H. Gupta and Z. Kalajzic, "Effect of low-frequency mechanical vibration on orthodontic tooth movement," *Am J Orthod Dentofacial Orthop*, vol. 148, no. 3, pp. 440-449, 2015.
- [39] T. Cheung, J. Park and D. Lee, "Ability of mini-implant-facilitated micro-osteoperforations to accelerate tooth movement in rats," *Am J Orthod Dentofacial Orthop.*, vol. 150, no. 6, pp. 958-967, 2016.
- [40] C. Yang, H. Jeon, A. Alshabab, Y. Lee, C. Chung and D. Graves, "RANKL deletion in periodontal ligament and bone lining cells blocks orthodontic tooth movement," *International Journal of Oral Science*, vol. 10, no. 1, 2018.
- [41] A. Ibrahim, S. Gudhimella, S. Pandravadra and S. Huja, "Resolving differences between animal models for expedited orthodontic tooth movement," *Orthod Craniofac Res.*, vol. 20, no. 1, pp. 72-76, 2017.
- [42] J. Chang, P. J. Chen, E. H. Dutra, R. Nanda and S. Yadav, "The effect of the extent of surgical insult on orthodontic tooth movement," *European journal of orthodontics*, vol. 41, no. 6, pp. 601-608, 2019.
- [43] J. Nguyen, S. Tang, D. Nguyen and T. Alliston, "Load regulates bone formation and Sclerostin expression through a TGF β -dependent mechanism," *PLoS One*, vol. 8, no. 1, p. e53813, 2013.

- [44] K. Oka, S. Oka, T. Sasaki, Y. Ito, P. Bringas, K. Nonaka and e. al, "The role of TGF-beta signaling in regulating chondrogenesis and osteogenesis during mandibular development," *Dev. Biol.*, vol. 303, pp. 391-404, 2007.
- [45] H. Seo and R. Serra, "Deletion of *Tgfb2* in *Prx1*-cre expressing mesenchyme results in defects in development of the long bones and joints.," *Dev. Biol.*, vol. 310, p. 304–316, 2007.
- [46] S. Tang and T. Alliston, "Regulation of postnatal bone homeostasis by TGFbeta," *Bonekey Rep*, vol. 2, no. 225, 2013.
- [47] C. Xu, X. Xie, H. Zhao, Y. Wu, J. Wang and J. Feng, "TGF-Beta Receptor II Is Critical for Osteogenic Progenitor Cell Proliferation and Differentiation During Postnatal Alveolar Bone Formation," *Frontiers in Physiology*, vol. 12, 2021.
- [48] C. Kirschneck, M. Bauer and J. Gubernator, "Comparative assessment of mouse models for experimental orthodontic tooth movement," *Sci Rep*, vol. 10, 2020.
- [49] N. S. Dole, C. S. Yee, C. M. Mazur, C. Acevedo and T. Alliston, "TGFβ Regulation of Perilacunar/Canalicular Remodeling Is Sexually Dimorphic," *J Bone Miner Res.*, vol. 35, no. 8, pp. 1549-1561, 2020.
- [50] X. Yao, S. M. Carleton, A. D. Kettle, J. Melander, C. Phillips and Y. Wang, "Gender-dependence of bone structure and properties in adult osteogenesis imperfecta murine model," *Ann Biomed Eng*, vol. 41, no. 6, pp. 1139-1149, 2013.
- [51] C.-Y. Ko, D. H. Seo and H. S. Kim, "Deterioration of bone quality in the tibia and fibula in growing mice during skeletal unloading: gender-related differences," *J Biomech Eng*, vol. 133, no. 11, 2011.

- [52] E. Seeman, "Sexual Dimorphism in Skeletal Size, Density, and Strength," *The Journal of Clinical Endocrinology and Metabolism*, vol. 86, no. 10, pp. 4576-4584, 2001.
- [53] N. Hart, S. Nimphius, T. Rantalainen, A. Ireland, A. Siafarikas and R. U. Newton, "Mechanical basis of bone strength: influence of bone material, bone structure and muscle action," *J Musculoskelet Neuronal Interact*, vol. 17, no. 3, pp. 114-139, 2017.
- [54] C. Chen, L. Wang, U. Tulu, M. Arioka, M. M. Moghim, B. Salmon, C.-T. Chen, W. Hoffmann, J. Gilgenbach, J. B. Brunski and J. A. Helms, "An osteopenic/osteoporotic phenotype delays alveolar bone repair," *Bone*, vol. 112, pp. 212-219, 2018.

Publishing Agreement

It is the policy of the University to encourage open access and broad distribution of all theses, dissertations, and manuscripts. The Graduate Division will facilitate the distribution of UCSF theses, dissertations, and manuscripts to the UCSF Library for open access and distribution. UCSF will make such theses, dissertations, and manuscripts accessible to the public and will take reasonable steps to preserve these works in perpetuity.

I hereby grant the non-exclusive, perpetual right to The Regents of the University of California to reproduce, publicly display, distribute, preserve, and publish copies of my thesis, dissertation, or manuscript in any form or media, now existing or later derived, including access online for teaching, research, and public service purposes.

DocuSigned by:

Jasmine Faldu

681B950DBEE64FE...

Author Signature

5/9/2022

Date